Towards a More Robust Salmon: Expanding the CRISPR Toolbox with Base Editing and Cas12, and Targeting Gene Regulatory Elements using the Zebrafish Model Species

Silje Broll

Master of Science in Biology - Aquaculture Biology
Department of Biological Sciences, University of Bergen
June 2023

Supervisors:
Ståle Ellingsen and Dorothy Jane Dankel, Department of Biological Sciences, University of Bergen
Rolf Brudvik Edvardsen and Mari Raudstein, Institute of Marine Research

Acknowledgements

First and foremost, I would like to thank the Institute of Marine Research and for being part of the TUNESAL project during this thesis.

My supervisors have been Ståle Ellingsen and Dorothy Jane Dankel at UiB, and Rolf Brudvik Edvardsen and Mari Raudstein at IMR. My sincerest thanks goes to Ståle Ellingsen, Rolf Brudvik Edvardsen and Mari Raudstein for the close follow-up and guidance throughout the whole period. A special thanks to Mari Raudstein for helping along all lab-work, through numerous obstacles and having countless discussions regarding different approaches. You have been there every step of the way and I am infinite grateful for your support and guidance. I would also like to thank Elsa Denker for helping during the lab work regarding bioanalyzer at UiB and Morten Barvik for help with zebrafish injections.

I would like to thank Mari Raudstein for MiSeq preparations and Erik Kjærner-Semb for help with MiSeq data. A huge thanks goes to Bjørnar Skjold for excellent help prior to zebrafish injections and husbandry, together with the staff at IMR Matre for husbandry of salmon.

Lastly, I would thank my fellow students, friends and family for endless support and encouragement during this year.

Bergen, June 2023
Silje Broll

Summary

The aquaculture industry needs to further increase the salmon production to meet the rising demand for food. However, the industry faces sustainability challenges including diseases. It is possible that some of these challenges can be overcome by increasing the expression of immune-related proteins, making a more robust salmon. This may be achieved by modifying regulatory elements that influence the mRNA stability, using CRISPR technology. To investigate the effect of regulating mRNA stability, we conducted injection experiments in zebrafish. Four different experiments were performed including KO of microRNA (miR) and miR target sites in two immune genes, *ifng* and *myd88*. All injections were performed together with gRNA targeting *slc45a2*, used as a marker gene for visual confirmation. KO of the *ifng* target site using Cas12 displayed a very high mutation rate. These findings from the zebrafish experiments can be applied to future studies on salmon, revealing the effect of KO of the *ifng* target site in salmon. KO of the *myd88* target site using Cas9 was successful, but even if *myd88* gRNA was very efficient, showing over 80% mutation rate at target site, the effect could not be evaluated by qPCR. However, KO of the *myd88* target site led to degradation of RNA, possibly caused by increased level of the Myd88 protein. We also aimed to expand the CRISPR toolbox for gene editing in salmon by injecting a base editor along with Cas9 to convert a C into T, inducing a stop codon (TAG) in *slc45a2*. This conversion was achieved with very high efficiency, as several samples displayed over 80% correct base conversion. Notably, base editing has not been previously reported in salmon. The second injection performed in salmon involved Cas12 KO and KI of an ODN template in *slc45a2*, resulting in insertion of FLAG sequence by HDR. MiSeq deep sequencing revealed that both KO and KI were highly efficient in this study, and this has not been reported before. In conclusion, base editing and Cas12 have for the first time been demonstrated in salmon and will be important tools for further studies using gene editing.

Contents

1 Abbreviations

A	Adenine
ABE	Adenosine Base Editor
BER	Base Excision Repair
C	Cytosine
Cas9	CRISPR associated protein 9
Cas12	CRISPR associated protein 12
CBE	Cytosine Base Editor
cDNA	complementary DNA
CRISPR	Clustered Regulatory Interspaced Short Palindromic Repeats
crRNA	CRISPR RNAs
Ct	Cycle threshold
DNA	DeoxyriboNucleic Acid
dpf	days post fertilization
DSB	Double strand break
elf1a	elongation factor-1 alpha
G	Glycosine
gRNA	guide RNA
HDR	Homology Directed Repair
hpf	hours post fertilization
ifng	interferon gamma
IMR	The Institute of Marine Research
JAK1	Janus Kinase 1
JAK2	Janus Kinase 2
KI	Knock In
KO	Knock Out
miR	micro RNA
mRNA	messenger RNA
myd88	myeloid differentiation factor 88
nCas9	nickase Cas9
NC	Negative Control
NHEJ	Non-Homologous End Joining
NRT	Non-Reverse-Transcription control
ODN	Oligonucleotide
PAM	Protospacer Adjacent Motif

PCR	Polymerase Chain Reaction
qPCR	quantitative Polymerase Chain Reaction
RIN	RNA Integrity Number
RNA	RiboNucleic Acid
RNP	RiboNucleoProtein
slc45a2	solute carrier family 45 member 2
SNR	Single Nucleotide Replacement
STAT 1	Signal Transducer and Activator of Transcription protein 1
STAT 2	Signal Transducer and Activator of Transcription protein 2
T	Thymine
TAE buffer	Tris-Acetate EDTA buffer
TALEN	Transcription Activator-Like Effector Nucleases
TLR	Toll-Like Receptor
tracrRNA	trans-activating crispr RNA
tuba1c	tubulin alpha 1c
U	Uracil
UiB	University in Bergen
UTR	UnTranslated Region
WT	Wild Type
ZFN	Zinc Finger Nucleases

2 Introduction

2.1 Aquaculture

In a world where the demand for food is increasing, aquaculture has emerged as a vital part of the solution. As the need for food increases, so does the urgency for higher protein production. In this regard, salmon, being among the most important aquaculture species, stands out as a nutritious source of protein. Aquaculture has been the fastest growing food production sector over several decades (Garlock et al., 2020), and in 2020 aquaculture stood for 89% of the seafood made for human consumption (FAO, 2022). Norway is the world's largest producer of salmon (Iversen et al., 2020), but the industry faces several sustainability challenges, including lice infestations, escapees and diseases that adversely impact the fish. Overcoming these challenges becomes imperative to enable increased production in line with the United Nations sustainable development goals number 14, which calls for the conservation and sustainable use of the oceans, seas, and marine resources for sustainable development.

2.2 Immune system, welfare and disease

Ensuring sustainable increases in salmon production is crucial to prioritize welfare without compromising it (Hvas et al., 2021). Given the environmental factors and infection pressure faced by farmed salmon, a strong immune system becomes essential, as infectious diseases are the leading cause of mortality in aquaculture (Pettersen et al., 2015). One approach to making salmon more robust is to increase the expression of immune-related proteins, as the combat against diseases or the response to them can be influenced by the activity of these genes. Increasing the expression of immune genes can be achieved by altering regulatory elements that influence the stability of mRNA.

2.3 CRISPR/Cas 9

Technology for performing gene editing has existed for a long time but falls short compared to clustered regulatory interspaced short palindromic repeats (CRISPR). There are four families of nucleases that are used in genome editing: conventional genome-editing techniques, meganucleases, zinc finger nucleases (ZFN), transcription activator-like effector nucleases (TALEN) and CRISPR/Cas9 (Gaj et al., 2013; Saber Sichani et al., 2022). CRISPR represents repeating sequences in prokaryotic DNA originally found in *Escherichia coli* by Dr. Nakata

(Ishino et al., 1987). This was several decades before CRISPR was developed as a reprogrammable gene-targeting tool in the bacterial immune system (Adli, 2018). CRISPR repeating sequences were separated by spacers that are random sequences and not repeating (Adli, 2018). As observed in the bacterial immune system, the spacers consist of sequences from phages incorporated when invaded, and synthesized into CRISPR RNA (crRNA). CRISPR, in conjunction with Cas enzyme, can identify and cleavage the DNA or RNA of the invader by utilizing sequence obtained from phages (Saber Sichani et al., 2022). This process involves the binding of crRNA to trans-activating CRISPR RNA (tracrRNA), resulting in destruction of foreign DNA (Brouns et al., 2008). The CRISPR-Cas system is dependent on crRNA, which works as a guide to block horizontal DNA transfer from phages (Marraffini & Sontheimer, 2008).

CRISPR-associated endonuclease 9 (Cas9) protein used in experiments is dependent on guide RNA (gRNA) for targeting specificity (Pickar-Oliver & Gersbach, 2019). gRNA serves as a fusion between tracrRNA and crRNA. The Cas9 enzyme needs a protospacer adjacent motif (PAM) sequence (5′-NGG-3′) on the 3′ end of the targeting sequence (Saber Sichani et al., 2022) to bind. gRNA can be designed after the location of the PAM sites and thereafter use the Cas protein as a cutting tool, 3 base pairs upstream from the PAM, to complete a DNA double strand break (DSB) (Pickar-Oliver & Gersbach, 2019). After the DSB is done by the CRISPR/Cas complex, the cell can repair the break by two different pathways. The non-homologous end joining (NHEJ) pathway, known for its error-prone nature, reconnects DNA strand by incorporating random nucleotide insertions or deletions. This process has the potential to induce frameshift mutations or gene knock-out (KO) (Saber Sichani et al., 2022). Homology-directed repair (HDR) will cause knock-in (KI) by using a template of interest to introduce a change in the genome, this could be point mutation or longer segment of DNA (Pickar-Oliver & Gersbach, 2019). CRISPR/Cas9 is currently used to make KO and small KI, e.g. using both symmetrical oligonucleotides (ODNs) and asymmetrical ODNs in salmon (Straume et al., 2021). The potential of this technology extends to the creation of sterile fish (Kleppe et al., 2017; Wargelius et al., 2016), fish resistant to diseases, parasites and other advantageous traits. These traits include improved feed conversion efficiency, as well as fish with enhanced levels of desired fatty acids, promoting overall fish health (Gratacap et al., 2019; Wargelius, 2019).

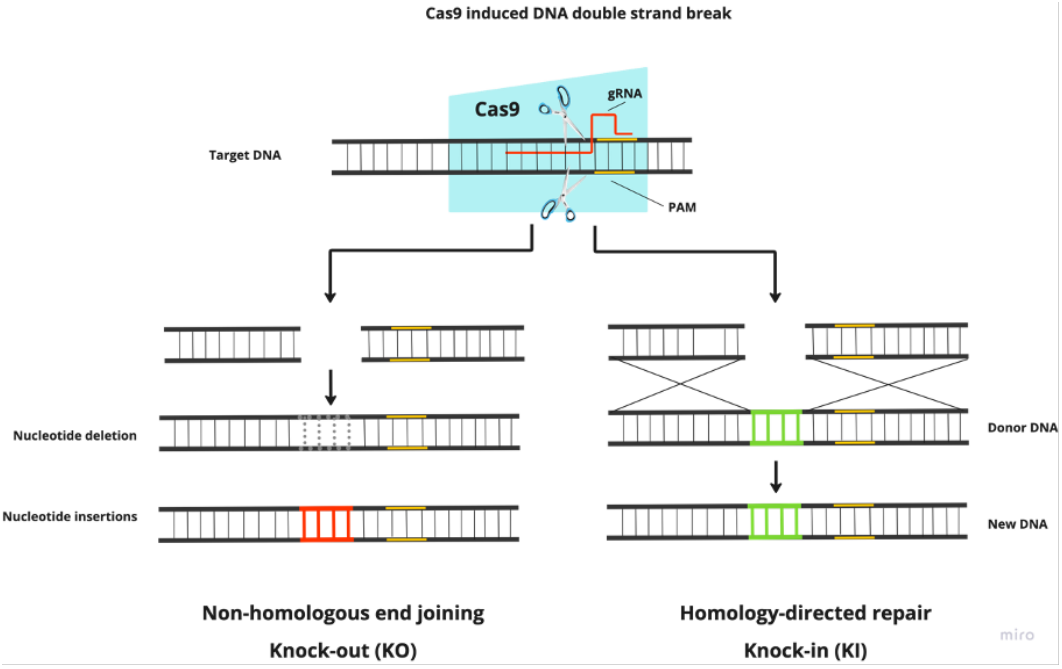

Figure 1: Repair pathways after DSB. The two different pathways (KO and KI) for the cell to repair DSBs. Figure made in miro.com.

2.3.1 Cas12

Since the discovery of Cas9, a number of other gene-editing tools have been discovered and now being utilized, including Cas12 and base-edit (Saber Sichani et al., 2022). Cas12, another RNA-guided endonuclease for gene editing, is guided by gRNA to make a staggered cut to the DNA (Anzalone et al., 2020). This gene editing tool might be beneficial when integrating DNA sequence of interest in precise location (Pickar-Oliver & Gersbach, 2019). Cas12 recognizes T-rich PAM sequence (5′-TTTV-3′, V is A, C, or G) on the 5′ end of the target sequence, compared to Cas9 which recognizes G-rich areas on the 3′end. This makes Cas12 preferable for targeting non-coding sequences with low GC-content. As Cas12 binds to different parts of the genome where Cas9 cannot, the diversity of gene editing is expanded.

2.3.2 Base edit

Single nucleotide replacement (SNR) represents small edits in the DNA that can change one amino acid or cause a stop codon. Using CRISPR to induce HDR and then “repair” with wanted sequence homologous to the CRISPR target site can be used to perform SNRs (Straume et al., 2021). Base edit is an alternative gene-editing tool to perform SNR that facilitates targeted nucleotide transformations with the benefit of reducing off-target effects.

Two types of base edit have so far been described, cytosine base editor (CBE) and adenine base editor (ABE) (Saber Sichani et al., 2022). Base editors consist of modified Cas9, so-called nickase Cas9 (nCas9), combined with a deaminase enzyme that convert the targeted base without inducing DSB, but rather makes a nick in one of the strands. In CBE, Cas9 and cytosine deaminase deaminates cytosine to uracil (C:U) in single-stranded DNA and nicks the corresponding strand. The strand with uracil base is then used as a template for the corresponding strand during mismatch repair of the nick, and changes G:A. Uracil is afterwards picked up by the replication mechanism in the cell as thymine which results in U:T transition (Kantor et al., 2020). Hence, CBE converts C-G base pair into T-A base pair. ABE shifts adenine base into guanine base, which results in converting A-T base pair into G-C base pair.

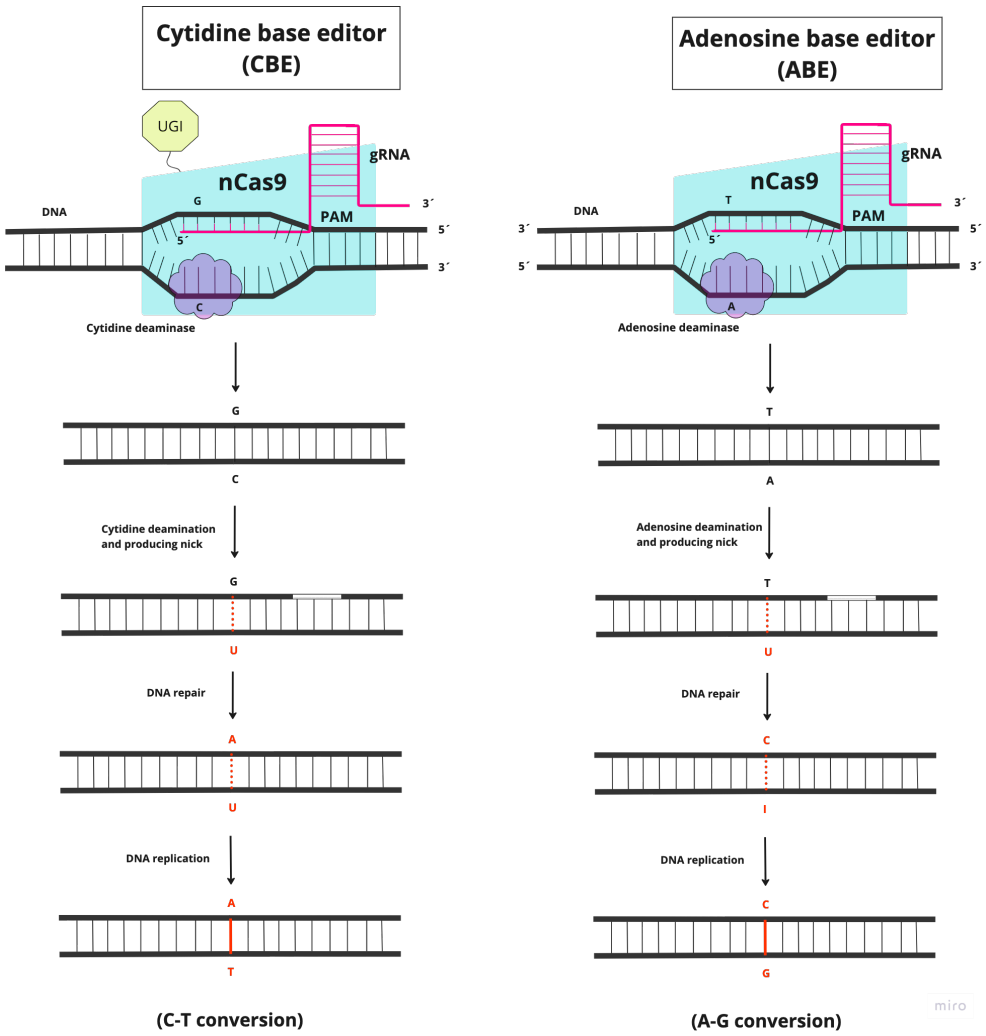

Figure 2: CBE and ABE base editors. Two types of base editors; CBE that convert C base into T and ABE that convert A base into G. Figure made in miro.com.

2.4 microRNA

One approach to make salmon more robust is by increasing expression of immune-related proteins. This can be achieved by increasing expression of immune genes or influencing their mRNA stability through modifying regulatory elements. One regulatory element is microRNA (miR) binding sites, which are conserved in the genome. miRs, which are short regulatory RNA molecules consisting of around 22 nucleotides, play a crucial role in post-transcriptional control of gene expression. They control the gene expression by binding to specific binding sites in a messengerRNA (mRNA) 3´UTR (Figure 3). miR can thereby silence the mRNA molecule in several ways: (i) cleavage of the mRNA strand; (ii) destabilize the mRNA; (iii) inhibit translation of the mRNA into protein (Bartel, 2018). Depending on the binding to the mRNA, gene silencing occurs based on complementary miR to the mRNA (Bartel, 2018). Each miR regulates a wide range of different transcripts and may have several target sites in some genes. The zebrafish *miR-223* have target sites in 4489 genes and *miR-144* have target sites in 7452 genes (targetscan.org).

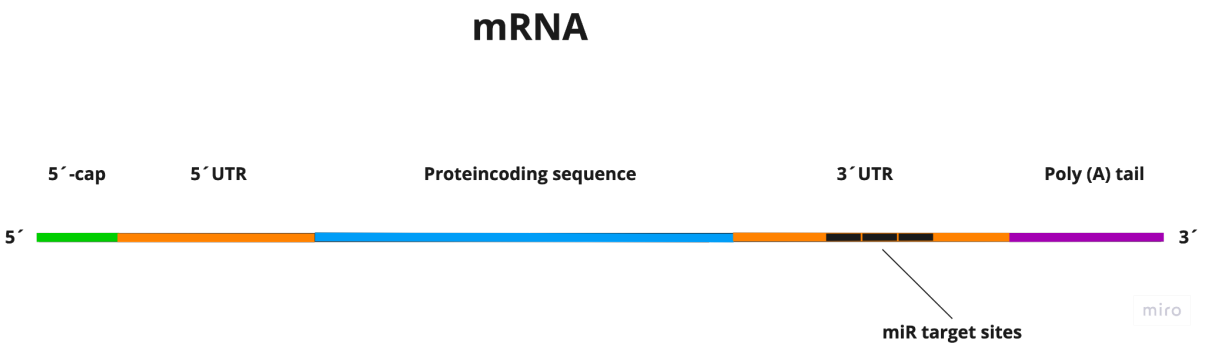

Figure 3: Overview mRNA. miR binds to target sites in 3´UTR of mRNA. Figure made in miro.com.

2.5 Immune genes *ifng* and *myd88*

Binding sites for *miR-223* and *miR-144* are found in the 3´UTR´s of mRNA of the immune genes *interferon gamma* (*ifng*) and myeloid differentiation factor 88 (*myd88*), respectively. *myd88* is an adaptor protein in Toll-like receptor (TLR) signaling pathways, which plays a central role in the immune system's recognition of invading pathogens (Takeda & Akira, 2004). In a study by van der Vaart et al. (2013), the first zebrafish mutant with a truncated version of *myd88* was examined. The findings revealed that the immune-compromised mutant exhibited reduced survival and higher vulnerability for some pathogens (*Edwardsiella tarda* and *Salmonella typhimurium*). This was due to the dependence of the pro-inflammatory cytokine

Il1b on *myd88* signaling during bacterial infections. Another important gene in the immune system, *ifng*, plays a significant role activating viral immunity through phosphorylation of Janus kinase 1 and 2 (JAK1 and JAK2). This will in turn activate the signal transducer and activator of transcription proteins 1 and possible 2 (STAT1 and STAT2). This pathway influences the transcription of genes essential for defense against infections (Grimholt et al., 2020). By editing target genes associated with the immune system, gene editing has the potential to induce wanted genotypes within one generation time (Ruan et al., 2017), increasing robustness in fish.

2.6 Zebrafish as a model for Atlantic Salmon

Testing new genome editing technology in salmon can be time-consuming and expensive due to the long generation time and reduced availability of eggs in large parts of the year. Therefore, using zebrafish (*Danio rerio*) first for testing and implementation of new approaches can be very beneficial. Zebrafish belong to a monophyletic group, Teleostei infraclass, thought to have arisen 340 million years ago (Howe et al., 2013), and introduced as a model organism by George Streisinger in 1970-1980 (Streisinger et al., 1981). Over the last decades, the zebrafish have become an essential model for a variety of studies in biomedicine, developmental biology, genetics, behavior, and physiology (Parichy et al., 2009). Other benefits of using zebrafish as a model is their transparency and rapid development. As the zebrafish embryo hatch between 48 to 72 hours post fertilization (hpf) into a larva, most major organs will be visible together with pigmentation, and therefore make them easy to study (Parichy et al., 2009). At 24 hpf, the embryos build up an immune response towards microbial infections (Herbomel et al., 1999).

2.7 Aims of the study

This thesis focuses on creating a more robust salmon by implementing new CRISPR strategies in salmon, and utilizing zebrafish as a model for pre-testing novel strategies.

The first aim of this study is:

- Further develop CRISPR technology in salmon by
    - establishing base editing as a method for defined single nucleotide replacement
    - implementing the use of Cas12 to broaden specter of possible target sites in the salmon genome

The second aim of this study is:

- Edit microRNAs and microRNA binding sites in zebrafish to increase expression of
    - *ifng*
    - *myd88*

3 Materials and methods

3.1 gRNA design

The target genes *ifng* and *myd88* were chosen based on their association with the immune system, having early expression and few miR binding sites. The gene sequences for *ifng* and *myd88*, together with their associated miR, *miR-144* and *miR-223*, were imported to Geneious Prime software for designing gRNA. CHOPCHOP (chopchop.cbu.uib.no) was used to detect PAM sites and cut sites together with the built-in CRISPR analyzing tool in Geneious. We attempted two approaches to disrupt the miR target site. The first approach was to design a gRNA to cut in the center of the miR target site (Figure 4 a) + c)), mutating it and therefore limiting the possibility for the miR to bind. The second approach was to design two gRNAs to cut on both the left and right (L+R) side of the miR target site, aiming to remove the entire site (Figure 4 b) + d)). Additionally, two gRNAs were designed to cut on both sides of the miR genes itself to KO the entire miR gene (Figure 4 e) + f)). All gRNAs were BLASTed against the zebrafish genome assembly to limit off-target effects. The gRNA sequences and the corresponding nuclease can be found in Table 1.

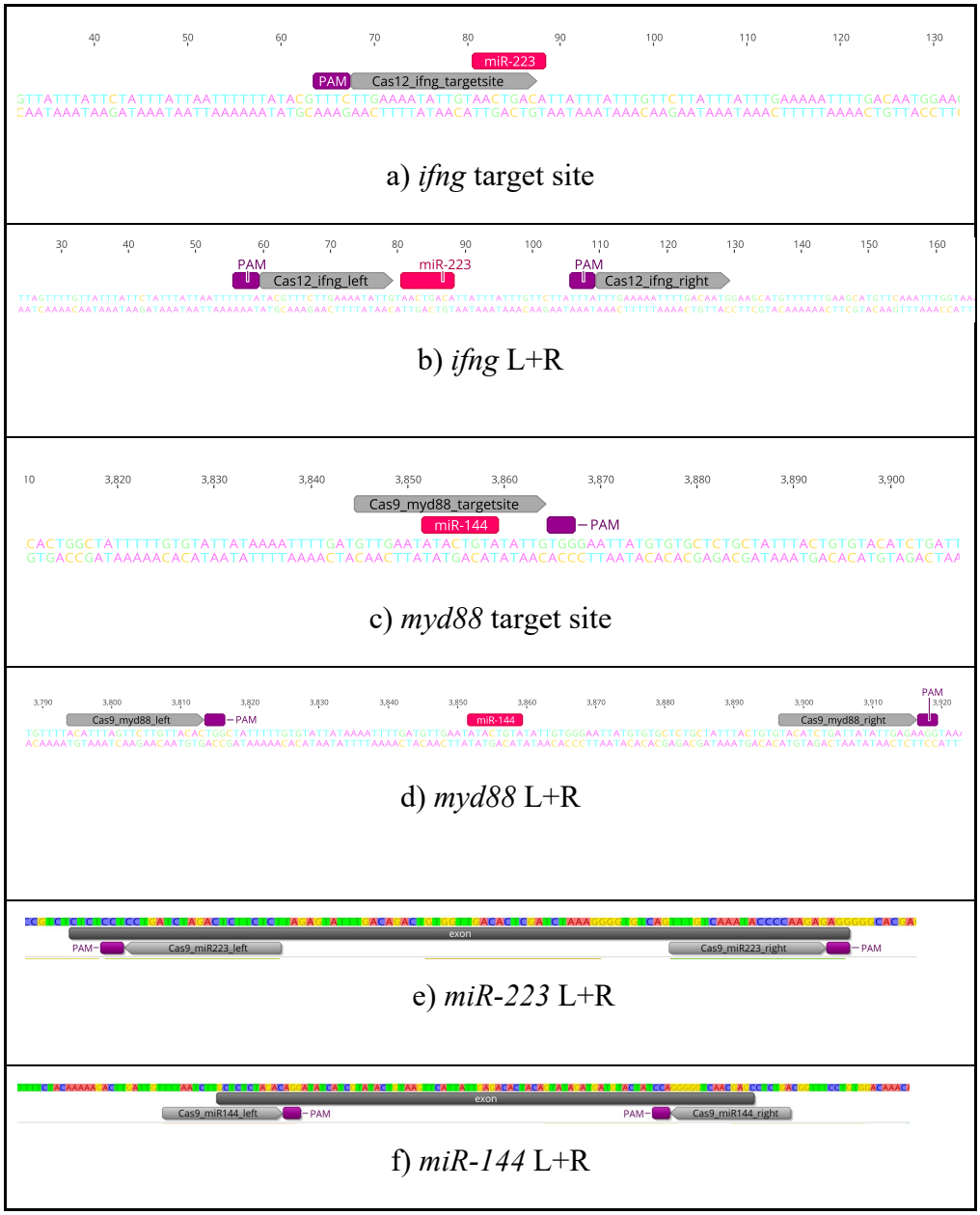

Figure 4: gRNA used for zebrafish injections. gRNA colored in gray and PAM sites colored in purple. a) + b) The gray box labeled miR-223 is the miR target site in the 3´UTR of *ifng* mRNA. c) + d) The gray box named miR-144 is the target site in the 3´UTR of *myd88* mRNA. e) The dark gray box is the exon coding for *miR-223*. f) The dark gray box is the exon coding for *miR-144*. Pictures are taken from Geneious Prime software.

Table 1: Sequences for the different gRNAs. gRNAs with associated Cas protein and sequence. PAM sites are underlined.

gRNA	Cas protein	Sequences (5´-3´)
*ifng*_targetsite	Cas12	TTTCTTGAAAATATTGTAACTGAC
*ifng*_targetsite_L	Cas12	TTTATACGTTTCTTGAAAATATTG
*ifng*_targetsite_R	Cas12	TTTATTTGAAAAATTTTGACAATG
*myd88*_targetsite	Cas9	GTTGAATATACTGTATATTGTGG
*myd88*_targetsite_L	Cas9	ACATTTAGTTCTTGTTACACTGG
*myd88*_targetsite_R	Cas9	TACATCTGATTATATTGAGAAGG
*miR-223*_L	Cas9	CCTCCTGATCTAGACTCTTCTCT
*miR-223*_R	Cas9	TTTGTCAAATACCCCAAGAGAGG
*miR-144*_L	Cas9	TTTAATCTTGCTCTCTAGACAGG
*miR-144*_R	Cas9	CAGAGGCTCGTTGACCCCCTGG
albino1	Cas9	GGCTCAGATCATCGTGGGGGCGG

gRNAs for *ifng* were ordered from Integrated DNA Technologies (Leuven, Belgium) complete and ready to use after adding the corresponding dH_2O volume. gRNAs for *myd88, mir-223, mir-144* and *slc45a2* (targeting albino, a marker gene for visual confirmation of gene editing) was made according to the protocol in Gagnon et al. (2014), where gRNA is produced from a DNA template. First step for annealing oligos consisted of mixing 1µl of gene-specific oligos (100µM), 1µl of constant oligo (100µM) and 8µl dH_2O together and run in a thermocycler. The thermocycler program started with 5 minutes at 95°C followed by a stage where the temperature decreased from 95°C to 85°C at a rate of 2°C/sec. In the final stage, the temperature decreased from 85°C to 25°C at a rate of 0.1°C/sec before a hold step at 4°C. The annealed oligos were mixed with a T4 master mix (Table 2). The 20µl product was then incubated at 12°C for 20 minutes.

Table 2: Contents of T4 DNA polymerase master mix.

Component	Volume (1 rxn)
dNTP (10mM)	2.5µl
10x NEB buffer 2.1	2µl
100x NEB BSA	0.2µl
T4 NEB DNA polymerase	0.5µl
dH_2O	4.8µl
Total	10µl

The DNA product was subsequently purified using the Qiagen PCR clean up kit, following the provided protocol apart from using a 30µl dH_2O elution volume. The concentration of the purified DNA product was measured using a NanoDrop 8000 spectrophotometer (ThermoFisher Scientific). To verify the product´s correct size, it was run on a 1% agarose gel (section 3.9).

The DNA was then transcribed into RNA with the use of T7 polymerase and HiScribe T7 Quick High Yield RNA synthesis kit (NEB). The master mix consisted of NTP buffermix and T7 polymerase. Input of the DNA product was 1000ng and dH_2O was added to a final volume of 30µl (Table 3). The samples were then incubated at 37°C for 16 hours.

Table 3: Contents of T7 polymerase master mix.

Component	Volume (1rxn)
dH_2O	x
NTP buffermix	10µl
Template DNA (up to 1000 ng)	x
T7 polymerase	2µl
Total	30µl

The next step in the gRNA synthesis was to remove the DNA template by a DNase treatment, where 20µl dH_2O and 2µl DNase I (RNase-free) was added to the 30µl product, and incubated at 37°C for 15 min. The RNA was cleaned up using RNeasy Mini Kit-columns (Qiagen) according to the manufacturer's protocol. The concentration of the gRNA was analyzed using a NanoDrop 8000 spectrophotometer (ThermoFisher Scientific), and then stored at -80°C.

3.2 Zebrafish administration and handling

Zebrafish were kept and handled at the Institute of Marine Research (IMR) at Nordnes, Norway. The adult zebrafish were kept at 28°C with a light regime of 14h light and 10h dark, and fed three times a day. Each 8L tank stored between 40 and 50 individuals. The day prior to fertilization, male and female zebrafish were placed in the same tank, but separated from the breeding area by a vertical mesh screen (Figure 5(1)). The following morning, the vertical block was removed, allowing the zebrafish to breed in the shallow part of the tank. The eggs would fall through a horizontal mesh screen to be collected in a chamber (Figure 5(2)). Approximately 15 min after removing the vertical block, the eggs were ready for collection. The eggs were rinsed with embryo medium (E3) (Table A2 + A3) and transferred onto a petri dish in preparation for injections.

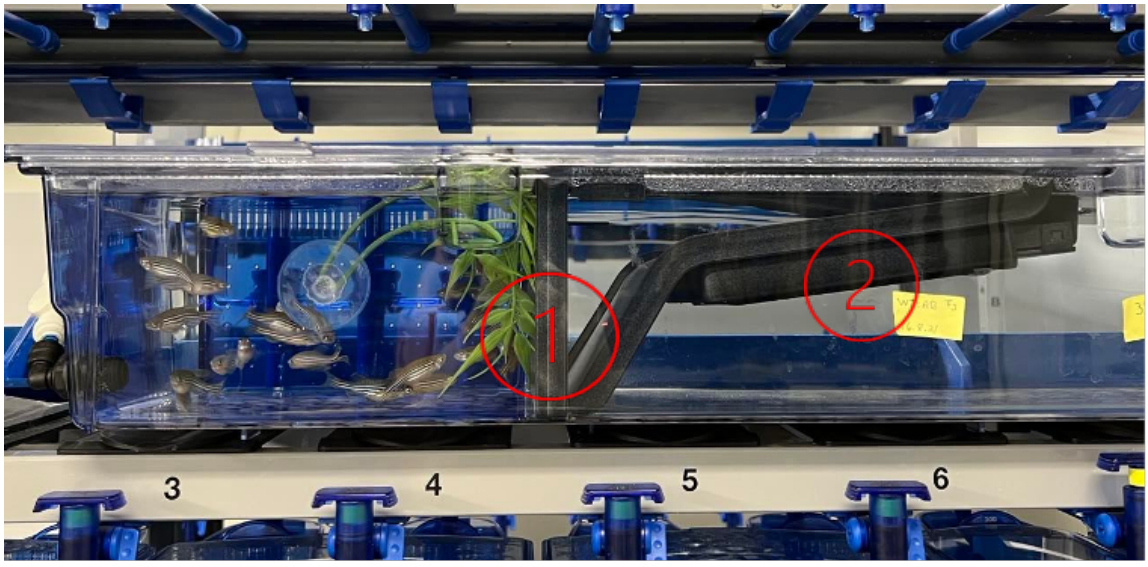

Figure 5: Zebrafish tank. Tank where female and male zebrafish were put together the day before injections. (1) Vertical mesh screen, removed to initiate breeding. (2) Chamber collecting eggs.

3.3 Zebrafish injections and sampling

A Nikon SMZ-645 stereomicroscope (Nikon, Japan) was used together with a FemtoJet 4i microinjector (Eppendorf, Germany) to perform the injections. Glass capillaries with an outer diameter of 1.0mm, inner diameter of 0.5mm and 10cm length (Sutter instrument) were heat-pulled by a PC-100 needle puller (Narishige, Japan) to form the needle used for injections. A volume between 2.5-3.5µl of injection mix was added into the needle before the tip was cracked open with a pair of tweezers. To ensure accurate injection volume, a Stage Graticules S8 Micrometer (Electron Microscopy Sciences, USA) 1mm ruler was used to calibrate the amount of injection mix injected into the eggs. The injected droplet had a diameter of 0.2mm, which is equivalent to 1nL injection mix.

For the *ifng* injection mix, two ribonucleoprotein (RNP) complexes were prepared and incubated for 15 minutes at room temperature before mixing and ready for injection. One RNP complex consisted of *ifng* gRNA along with Cas9 protein (1000ng/µl) (for injections done targeting *miR-223*) or Cas12 protein (for injections done targeting *ifng* target site) at a final concentration of 100ng/µl and dH_2O. The other RNP complex consisted of gRNA targeting the *slc45a2* gene (2777ng/µl) and Cas9 (1000ng/µl) at a final concentration of 100ng/µl along with dH_2O.

Similarly, two RNP complexes were prepared for the *myd88* injection mix and incubated for 15 minutes at room temperature before mixing and ready for injection. One RNP complex consisted of *myd88* gRNA and Cas9 protein (1000ng/µl) at a final concentration of 100ng/µl along with dH_2O. The other RNP complex consisted of gRNA targeting the *slc45a2* gene (2777ng/µl) and Cas9 protein (1000ng/µl) at a final concentration of 100ng/µl along with dH_2O.

Fertilized eggs were transferred in groups of approximately 50 individuals onto a petri dish containing agarose with canals fitting the eggs (Figure 6 (1)). The eggs were placed down in the agarose mold with a pipette tip to inhibit movement when injecting, and therefore increase injection efficiency. Injections were performed in the yolk of the egg and took place before the eggs reached the second cell stage, 45-60 min post fertilization. After injection, the eggs were washed out of the agar mold with E3 medium onto a new petri dish. Each petri dish contained roughly 50 injected eggs. The control groups were transferred directly from the same egg batch

as the injected groups into separate petri dishes, following an equal duration outside the tank before incubation. The eggs were incubated, with daily husbandry, at 28°C until 5 days post fertilization (dpf) before sampling. After 5 days, the larvae were anesthetized, and the most visual albino individuals were sampled together with controls. Both injected and controls were sampled on ethanol for DNA extraction and RNAlater for RNA extraction.

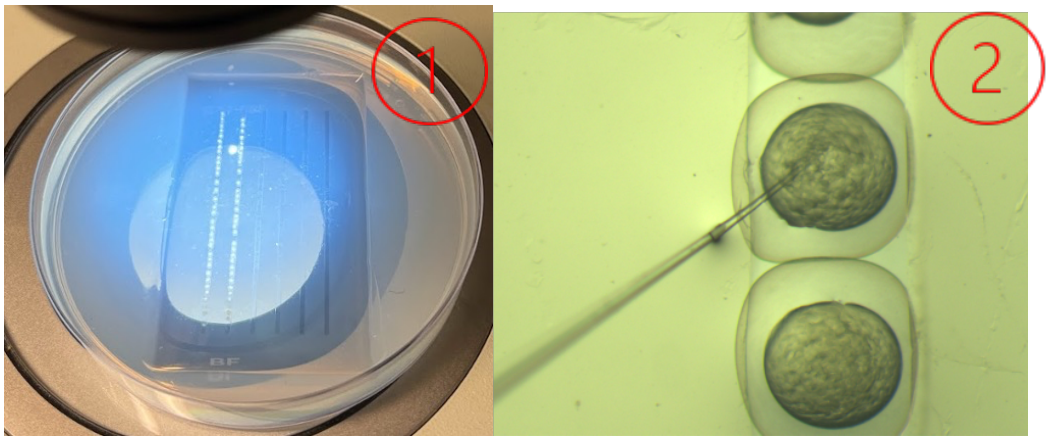

Figure 6: Different parts of zebrafish injections. (1) Agarose mold with eggs fitting the channels ready for injections. (2) Needle injecting injection mix into the yolk of zebrafish egg.

3.4 Salmon injections and sampling

Eggs and sperm from salmon were picked up from MOWI at Askøy, Norway and stored on ice. Fertilizing was done in glutathione to prevent chorion hardening, which was made by adding 0.15g Glutathione (Sigma-Aldrich, USA) to 1L MilliQ water. The pH was adjusted to the optimal level of 10 by adding NaOH. If the pH exceeded 10, HCl was added to lower the pH into the desired range. Glutathione was stored in the fridge or on ice to keep cold (6-8°C) until fertilization. Sperm from two different individuals were transferred with a plastic pipette into the egg batch from one female and mixed. Glutathione was added after 1 min, and the injections were performed after about 3 hpf. Injections were done at the IMR at Matre, Norway. 50 fertilized eggs were transferred to a tray containing individual spots for each egg. The eggs were gently rotated using a pipette tip to ensure that the cells were orientated upwards, facilitating easier injections. Injections were done using an Olympus SZX10 Stereo Microscope (Olympus, Japan) together with a FemtoJet 4i microinjector (Eppendorf, Germany). Capillaries used for the injections had a length of 10cm, with outer diameter of 1.0mm and inner diameter of 0.5mm that got heat-pulled by needle puller PC-100 (Narishige, Japan).

Injection mix for base edit was made by Mari Raudstein and contained AncBE4max base editor mRNA (3130ng/µl) (Table A4) with a final concentration of 300ng/µl, albino1 gRNA (2183ng/µl) (Table 1) with a final concentration of 100ng/µl and dH_2O. Injection mix for Cas12 FLAG KI non-target template was also made by Mari Raudstein, and consisted of L.b Cas12 protein ultra (10µg/µL) with a final concentration of 100ng/µL, Alb_ex1 crRNA (100µM) (Table A4) with a final concentration of 100ng/µL, template Cas12_alb_nont_90PAM (100µM) with a final concentration of 1.5µM and dH_2O. Injection mix for Cas12 FLAG KI target template consisted of L.b Cas12 protein ultra (10µg/µL) with a final concentration of 100ng/µL, Alb_ex1 crRNA (100µM) (Table A4) with a final concentration of 100ng/µL, template Cas12_alb_target_90PAM (100µM) with a final concentration of 1.5µM and dH_2O. All injection mixes were prepared fresh prior to the injections.

After injections, the eggs were transferred to hatching trays. The eggs were kept at 6°C with no light until sampling at ~700 day degrees. The husbandry was carried out by the staff at IMR Matre until sampling. On the day of sampling, the fish were anesthetized using Finquel along with a buffer to maintain a neutral pH. The number of individuals sampled varied across groups depending on the abundance of the visual albino phenotype. Individuals with the albino phenotype were sampled in ethanol for subsequent DNA extraction.

3.5 DNA extraction

DNA extraction from zebrafish larvae and salmon fin clips was conducted following the protocol of the Qiagen DNeasy Blood & Tissue Kit (Qiagen, USA), except from the elution volume, which was set to 100µl. The final DNA concentration was measured on a NanoDrop 8000 spectrophotometer (ThermoFisher Scientific).

3.6 Sanger sequencing

3.6.1 PCR Q5 High-Fidelity DNA polymerase

Sanger sequencing was used to determine the effectiveness of the gRNA and determine which injected groups to proceed with for qPCR analysis. To check the gRNA effect, the target sites of interest were amplified using Q5 PCR. Individual master mixes (Table 4) were made for the different genes with corresponding primers (Table A1). After adding the master mix to the

different samples, they were run through a thermocycling program (Table 5). The PCR product was assessed on 1% agarose gel to verify if the amplification was successful (section 3.9).

Table 4: Contents of Q5 PCR master mix.

Component	Volume (1 rxn)
Q5 5x Reaction Buffer	2µl
Q5 HF DNA Polymerase	0.1µl
dNTPs (10µM)	0.2µl
F primer (10µM)	0.5µl
R primer (10µM)	0.5µl
dH_2O	5.7µl
Template	1µl
Total	10µl

Table 5: Q5 PCR thermocycling program.

Stage 1	Stage 2			Stage 3	
98°C	98°C	65°C	72°C	72°C	4°C
30sec	10sec	20sec	30sec	3min	∞
x1	x30			x1	

3.6.2 BigDye PCR

The PCR product was purified by ExoSAP-IT PCR Product Cleanup (ThermoFisher Scientific). The cleanup removes excess primers and nucleotides. 5µl of post PCR product was mixed with 2µl of ExoSAP-IT reagent, and incubated at 37°C for 15 min followed by 80°C for 15 min. The final step to prepare the samples for sanger sequencing was by using the BigDye Terminator v3.1 Cycle Sequencing Kit (ThermoFisher Scientific). The master mix was combined with a 1µl template from the cleaned-up PCR product (Table 6). The resulting 10µl

product was run in a thermocycler using the program in Table 7. Following completion of the program, 10µl of dH_2O was added, and the sample was sent to the DNA Sequencing Lab at the University of Bergen.

Table 6: Contents of BigDye PCR master mix.

Component	Volume (1rxn)
BigDye v3.1 Reaction Mix	1µl
5X Sequencing buffer	1µl
1mM reversed primer	3.2µl
Template	1µl
dH_2O	3.8µl
Total	10µl

Table 7: PCR cleanup thermocycling program.

Stage 1	Stage 2			Stage3
96°C	96°C	50°C	60°C	4°C
5min	30sec	30sec	45sec	∞
x1	x25			

3.7 MiSeq

As a supplement to sanger sequencing, DNA from injected groups with gRNA targeting *ifng* and *myd88*, except from *myd88*_targetsite_L+R, were prepared for Illumina MiSeq deep sequencing. All preparations of the MiSeq library were done by Mari Raudstein as in Gagnon et al. (2014), using Q5 enzyme instead of Phusion. MiSeq was performed at the IMR in Arendal, Norway. After MiSeq, the Fastq files were filtered by Erik Kjærner-Semb using Cutadapt (Martin, 2011) and sorting the read counts into different categories.

3.8 qPCR

3.8.1 RNA extraction

RNA was extracted from zebrafish individuals or pools using the RNeasy Mini kit (Qiagen, USA) according to the protocol. Disruption and homogenization were done by vortexing the tissue in 600µl Buffer RLT, and the RNA was eluted in 30µl. RNA concentrations were measured on a NanoDrop 8000 spectrophotometer (ThermoFisher Scientific). The RNA samples were kept on ice from the elution step until the measurement of the concentrations. Subsequently, the samples were transferred to a -80°C freezer for storage.

3.8.2 Agilent Bioanalyzer

The quality of the extracted RNA product was assessed using the Bioanalyzer RNA 6000 Nano Assay (Agilent Technologies, USA) and the 2100 Bioanalyzer Instrument (Agilent Technologies, USA), following the manufacturer's protocol. The resulting RNA Integrity Number (RIN) value was obtained, which gives an indication of the quality of the RNA.

3.8.3 cDNA synthesis

The SuperScript VILO cDNA Synthesis Kit (ThermoFisher Scientific) was used to generate cDNA from the extracted RNA. A 10µl reaction was prepared for each sample, an exception from the protocol´s specified 20µl. This adjustment was made to minimize the consumption of reagents. A master mix was made for all the samples, including a negative control (NC), and consisted of 2µl 5X VILO Reaction Mix and 1µl 10X SuperScript Enzyme Mix for each sample. Input of RNA was set to 100ng. To achieve a final reaction volume of 10µl, dH_2O was added alongside the master mix as per the volume requirements determined by the RNA concentration in each of the different samples. The NC was prepared with dH_2O instead of RNA template and no reverse-transcription control (NRT) was prepared with dH_2O instead of 10X SuperScript Enzyme Mix. The samples were spun down before incubation according to Table 8 below. After the incubation, the samples were spun down and diluted 1:5 (added 40µl dH_2O) before being stored at -20°C.

Table 8: cDNA incubation program.

Stage 1	Stage 2	Stage 3	Stage 4
25°C	42°C	85°C	4°C
10min	60min	5min	∞

3.8.4 Dilution curve/primer validation

A dilution curve was performed to assess the efficiency of the primers targeting the gene of interest (*myd88*), as well as two housekeeping genes (*elf1a* and *tuba1c*) used as control genes (Xu et al. 2016). A cDNA pool was made by adding 5µl of each sample, and was further diluted in series; 1:10, 1:20, 1:40, 1:80, 1:160. Triplicates were made for each dilution value to observe any potential variation in pipette usage (Table 9). The NRT had a dilution of 1:10. A master mix was prepared for the three individual genes (*myd88*, *elf1a* and *tuba1c*) and consisted of 12.5µl of Sybr Green supermix, 0.5µl of forward primer and 0.5µl reversed primer (Table A1) together with 6.5µl dH_2O was added to each well. The qPCR plate was sealed with a MicroAmp Optical Adhesive Film (ThermoFisher Scientific) before being vortexed, centrifuged and run in QuantStudio 5 (ThermoFisher Scientific), using program in Table 10. The efficiency for the primers was calculated by Design and Analysis Software in a standard curve plot, where the average cycle threshold value (Ct-value) was plotted against log10 for the different dilutions. A linear regression displayed the slope and the primer efficiency (Eff%) was shown.

Table 9: Plate setup for dilution curve and primer validation. Overview of qPCR plate with the different dilutions, including NRT and NC at the bottom of the plate.

	1	2	3	4	5	6	7	8	9	10	11	12
A	d1:10	d1:10	d1:10	d1:10	d1:10	d1:10	d1:10	d1:10	d1:10			
B	d1:20	d1:20	d1:20	d1:20	d1:20	d1:20	d1:20	d1:20	d1:20			
C	d1:40	d1:40	d1:40	d1:40	d1:40	d1:40	d1:40	d1:40	d1:40			
D	d1:80	d1:80	d1:80	d1:80	d1:80	d1:80	d1:80	d1:80	d1:80			
E	d1:160	d1:160	d1:160	d1:160	d1:160	d1:160	d1:160	d1:160	d1:160			
F	NRT	NRT	NRT	NRT	NRT	NRT	NRT	NRT	NRT			
G	NC	NC	NC	NC	NC	NC	NC	NC	NC			
H												
		myd88			*elf1a*			*tuba1c*				

Table 10: qPCR incubation steps.

Step 1	Step 2		Step 3		Step 4
95°C	95°C	60°C	95°C	60°C	95°C
2min	15sec	25sec	15sec	1min	+0.15°C/s 1sec
x1	x40		x1		x1

3.8.5 qPCR of *myd88*

The cDNA samples were diluted 1:10 for the qPCR. Three different master mixes were made for the individual genes (*myd88, elf1a* and *tuba1c*) containing 6.25µl SYBR Green Supermix, 0.25µl forward primer, 0.25µl reversed primer and 3.25µl dH_2O for each sample. 10µl of the respective master mix were transferred to MicroAmp Optical 96-well Reaction plate (ThermoFisher Scientific) with automatic pipette. NTC and NC were included on the right side

of the plate. 2.5µl samples were added to the related wells manually (Table 11). The qPCR plate was sealed with a MicroAmp Optical Adhesive Film (ThermoFisher Scientific) before being vortexed, centrifuged and ready for qPCR run in QuantStudio 5 (ThermoFisher Scientific), using the program in Table 12.

Table 11: Plate setup for qPCR.

	1	2	3	4	5	6	7	8	9	10	11	12
A	1201	1202	1203	1201	1202	1203	1201	1202	1203	NRT	NRT	
B	1201	1202	1203	1201	1202	1203	1201	1202	1203	NRT	NRT	
C	1204	1205	1206	1204	1205	1206	1204	1205	1206	NRT	NRT	
D	1204	1205	1206	1204	1205	1206	1204	1205	1206	NRT	NRT	
E	1207	1208	1209	1207	1208	1209	1207	1208	1209	NRT	NRT	
F	1207	1208	1209	1207	1208	1209	1207	1208	1209	NRT	NRT	
G	1210	1211	1212	1210	1211	1212	1210	1211	1212			
H	1210	1211	1212	1210	1211	1212	1210	1211	1212			
		myd88			*elf1a*			*tuba1c*				

Table 12: qPCR incubation steps.

Step 1	Step 2		Step 3		Step 4
95°C	95°C	60°C	95°C	60°C	95°C
2min	15sec	25sec	15sec	1min	0.15°C/s 1sec
x1	x40		x1		x1

3.9 Gel electrophoresis

Gel electrophoresis were used to verify PCR product size. A 1% agarose gel was prepared by mixing 1g agarose with 100ml 1xTAE buffer. 5µl of GelRed was added to 80ml of the 1% agarose, which solidified after 30 minutes, resulting in final gel ready for sample loading. For sample loading, 1µl of PCR product, along with 1µl of GoTaq buffer and 3µl of dH_2O were loaded into the wells within the gel. Additionally, 1µl of DNA ladder (MassRuler) were loaded on each side as a reference. The electrophoresis gel was submerged in a 1xTAE buffer and connected to an electrical current. Electrophoresis was performed at 80V for 1h to separate the DNA fragment based on size. To verify the size of the DNA fragments, the gel was subjected to UV light using iBright CL1000 (ThermoFisher Scientific). This allowed visualization of the fragments in relation to the DNA ladder as a reference point.

4 Results

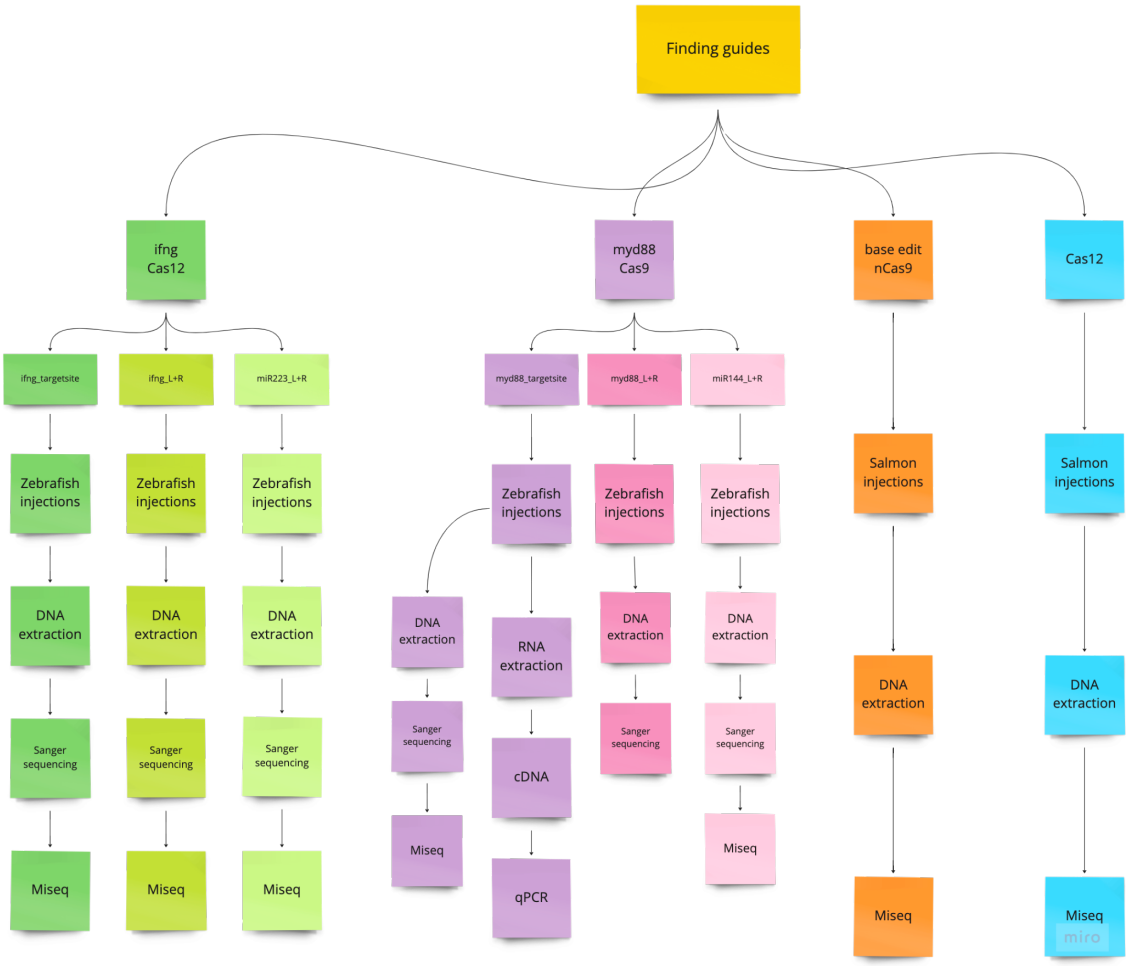

Figure 7: Flowchart over the different groups included in this thesis. Overview of the different steps during the experiment. Green and pink pathways display zebrafish, while orange and turquoise represent salmon. Samples in Table A5 are colored respectively to colors in the figure. Figure made in miro.com.

4.1 CRISPR technology development in salmon

For CRISPR technology development we have used gRNA targeting *slc45a2* (albino) as marker gene for visual confirmation, as used previously for technical development in salmon (Edvardsen et al., 2014; Straume et al., 2020; Straume et al., 2021). To identify *slc45a2*-mutants, individuals displaying an albino phenotype were selected by visual inspection.

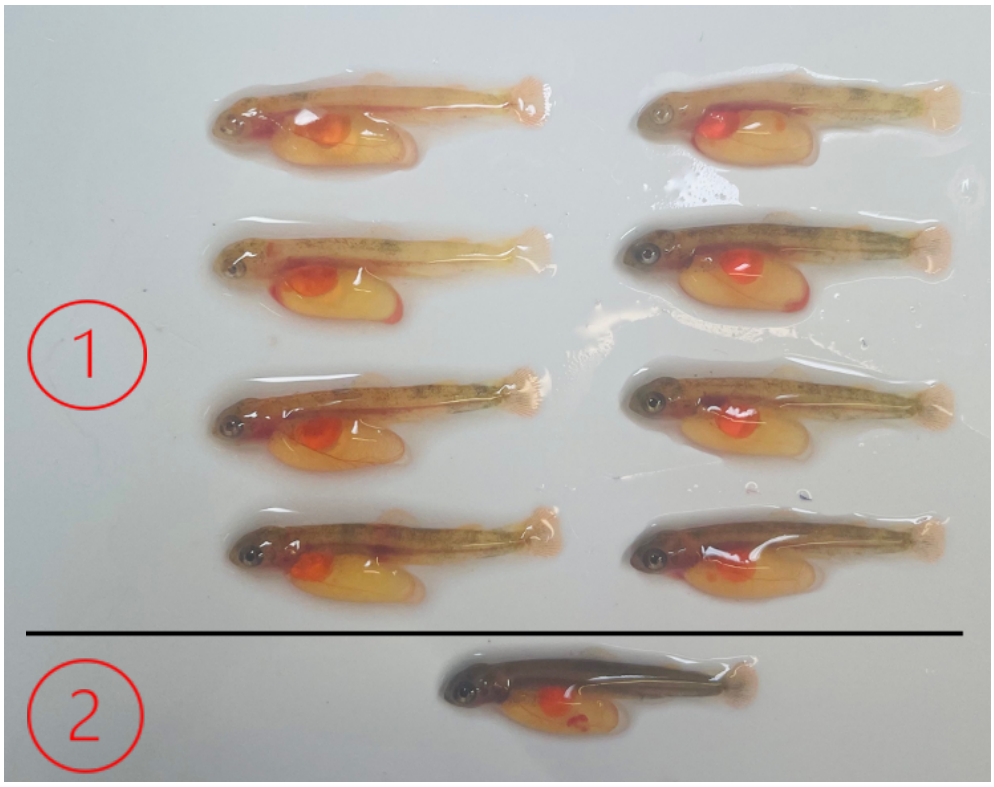

Figure 8: Albino and pigmented salmon larvae from injections of base editing. (1) Albino phenotype; (2) control. From base editing injections, eight individuals with albino phenotype were sampled (sample 6101-6108).

4.1.1 Base editing

We injected 700 Atlantic salmon eggs with the albino gRNA and the AncBE4max base editor mRNA. The eggs were kept in the dark in hatching trays for ~ 700 day degrees. Eight larvae with the albino phenotype were sampled (sample 6101-6108, Figure 8) and subjected to MiSeq deep sequencing to evaluate the efficiency of the injected base editor. The MiSeq results were divided into three different categories; (I) correct conversion, where the targeted C base was converted to a T base inducing stop codon (TAG); (II) wild type sequence (WT) where no change has occurred; (III) erroneous edits, which include all other instances apart from the two first groups (Table 13). Only sequence variants with 100 or more reads were included in our analyses. On average, the correct conversion efficiency of base editing was 66.5%, with the

highest observed individual efficiency of 89.1%, in sample 6101. WT sequences were observed at a low frequency in all samples except from sample 6108, where the individual had an equal amount of WT sequences and correctly converted C:T base. Erroneous edits from the MiSeq data include indels of both deletions and insertions, together with bystander and incorrect conversion (Figure 9).

Table 13: Correct conversion in base editing. Percentage of correct conversion (C:T), wild type (WT) and errors in base editing.

Sample	Correct conversion	WT	Errors
6101	89.1 %	3.5 %	7.3 %
6102	87 %	6.4 %	6.6 %
6103	59.8 %	16.6 %	23.5 %
6104	46.8 %	30.4 %	22.8 %
6105	85.9 %	7.1 %	7 %
6106	63 %	22.1 %	14.9 %
6107	64.3 %	22.6 %	13.1 %
6108	36.3 %	36.6 %	27.1 %

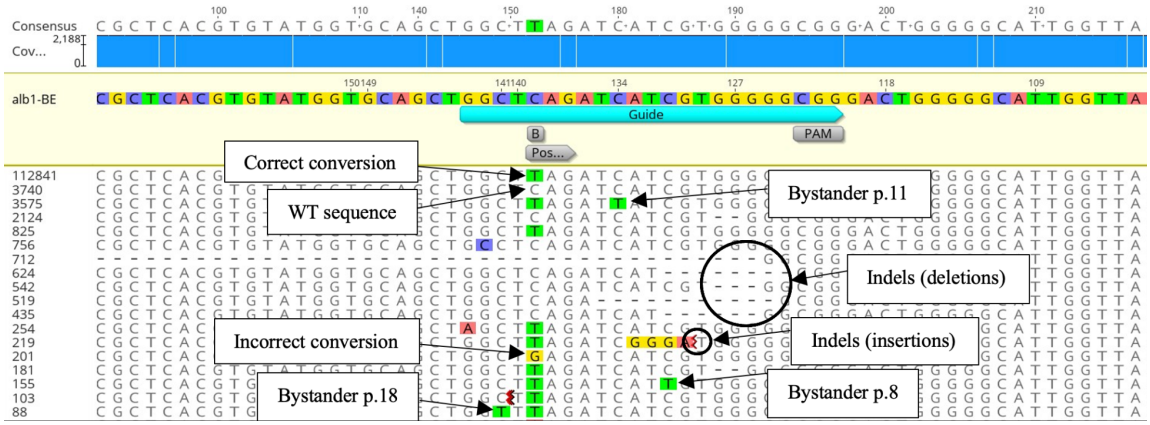

Figure 9: MiSeq result from base editing. Overview over different instances during base edit. Data from sample 6101 is shown. The numbers to the left of the sequences represent total reads of the specific sequence in that row. gRNA colored in turquoise. PAM site (CGG), target base (C) and possible stop codon (CAG) are all colored in gray. Figure taken from Geneious Prime software.

The most common type of erroneous edit was indels, with deletions occurring at an average rate of 7.5% (Table 14). A base editor should not make DSBs in the genomic DNA. However, the location of the deletions indicates that this had indeed occurred. Insertions, on the other hand, were rare with an average rate of 0.9% and ranged from inserting one to thirty bases across the samples.

Table 14: Indels errors from base editing. Percentage of the two groups of indels, insertions and deletions.

Sample	Insertions	Deletions
6101	0.3 %	4 %
6102	0 %	2.1 %
6103	0.4 %	6.7 %
6104	4.3 %	5 %
6105	0.3 %	3.8 %
6106	0.2 %	9.8 %
6107	1.3 %	7.3 %
6108	0.2 %	21 %

Bystander errors refers to unintended conversion of non-target C bases that get converted into T, resulting in an unintended C:T transition. These types of unintended conversions were most frequently observed at position 8 (p.8), 11 (p.11) and 18 (p.18) bases upstream of the PAM site (Figure 9). The highest frequency of bystander errors occurred at p.11, with an average of 2.5% (Table 15).

Table 15: Bystander errors from base editing. p.8, p.11 and p.18 refers to the number of bases from the PAM site.

Sample	p.8	p.11	p.18
6101	0.1 %	2.8 %	0 %
6102	0 %	2.2 %	0.1 %
6103	7.6 %	3.8 %	0.5 %
6104	1.2 %	3.4 %	6.1 %
6105	0.9 %	1.4 %	0.2 %
6106	0.4 %	3.2 %	0.2 %
6107	0.2 %	3.4 %	1.5 %
6108	0.4 %	1 %	0.3 %

The final group of errors observed was incorrect conversion, which occurs when the targeted base is converted into a different base other than T, such as G or A. These types of conversions were rare, with frequencies of 2.5% and 0.2%, respectively (Table 16).

Table 16: Incorrect conversions from base editing. Percentage of instances where target base was converted into an unwanted base G or A.

Sample	C:G	C:A
6101	0.2 %	0 %
6102	2 %	0.1 %
6103	5.1 %	0 %
6104	6.3 %	0.8 %
6105	0.4 %	0 %
6106	1.3 %	0.4 %
6107	0.8 %	0.2 %
6108	4.2 %	0.1 %

4.1.2 CRISPR/Cas12 KO and KI

Atlantic salmon eggs were injected targeting the pigmentation gene *slc45a2* for easy visual confirmation. To investigate both KO and KI at the same time we also included ODN templates in the injection mix. We used target (homologous to target sequence) and non-target (homologous to non-target sequence) ODN templates together with Cas12 protein and injected 568 and 754 embryos, respectively, to induce FLAG insert by HDR. FLAG is a commonly used artificial epitope used to tag proteins for capture and detection. Cas12 recognizes PAM sites (TTTV) on non-target strand and binds to the target strand (opposite strand of the one with PAM site). Only sequence variants with 100 or more reads were included in our analyses. Perfect HDR represent insertion of FLAG sequence with no indels. The percentage of perfect HDR was calculated by subtracting the number of WT reads from total reads, and then determining the proportion of instances where CRISPR occurred alongside perfect HDR. The average of FLAG insert was 4.6 % in all samples, while four samples had inserts with over 15% perfect HDR (Table 17). The sample with the highest occurrence had 54.9% FLAG inserts with perfect HDR (sample 7311). Imperfect HDR represents insertions of FLAG with various indels inside or at one or both sides of the inserted sequence (Figure 10). Such inserts represent HDR occurrence, but indicate errors to have arisen in the repair process. Imperfect HDR occurred 4.2% on average between all samples. Indels, categorized as KO, were the most frequent type of reads observed in all samples, except for one (sample 7311). On average, KO accounted for 57.8% of the reads.

Table 17: Perfect HDR, imperfect HDR and KO with Cas12 in salmon. Percentage of perfect HDR (FLAG insert), imperfect HDR (FLAG inserted, but with errors on the ends or in the middle) and KO (mutated reads). % Perfect HDR and % Imperfect HDR measured by subtracting wild type reads from total reads. KO reads measured from total reads - wildtype reads - imperfect reads - perfect reads. Sample 7201-7227 target. Sample 7301-7320 non-target.

Sample	% Perfect HDR	% Imperfect HDR	KO	Total reads
7201	0 %	0.8 %	56.6 %	39053
7202	0 %	6.3 %	73.3 %	35276
7203	0 %	0 %	83.9 %	36900
7204	0 %	12.3 %	62.7 %	35275

7205	2.3 %	4.3 %	80.7 %	24440
7206	0 %	0 %	87.1 %	39944
7207	0.4 %	0.3 %	89.9 %	46895
7208	0.6 %	0.6 %	87.5 %	25140
7209	0.3 %	0 %	83.2 %	35314
7210	0 %	2.6 %	84.1 %	30497
7211	0 %	0.8 %	80.2 %	33726
7212	0 %	0.7 %	58.9 %	37587
7213	0 %	0 %	54.2 %	42859
7214	0 %	13.2 %	60.9 %	30807
7215	0.4 %	1 %	78.1 %	51091
7216	0 %	0.8 %	68.3 %	37854
7217	0 %	0.7 %	75.2 %	45451
7218	0 %	13.9 %	65.5 %	39525
7219	17.4 %	0 %	46.7 %	38036
7220	26.6 %	5.2 %	43.1 %	36428
7221	0.5 %	1.7 %	71.6 %	36730
7222	0 %	0 %	64.5 %	41188
7223	1 %	0.4 %	51.6 %	48005
7224	0 %	0.6 %	67.1 %	40240
7225	1.4 %	0.9 %	61.4 %	36027
7226	0 %	3 %	54.6 %	44967
7227	34.3 %	0 %	41.5 %	28504
7301	4.1 %	6.7 %	58.2 %	37839
7302	27.8 %	0.5 %	63.9 %	41948

7303	0.5 %	1.9 %	82 %	50166
7304	14.7 %	2 %	57.4 %	23824
7305	0.5 %	6.1 %	42.2 %	47436
7306	3.6 %	2.3 %	46.9 %	44270
7307	0 %	4.8 %	55.6 %	36558
7308	0 %	16.5 %	44.5 %	39227
7309	0 %	14.8 %	58 %	32775
7310	0 %	0 %	61.6 %	30229
7311	54.9 %	4.2 %	26.7 %	33883
7312	0 %	22.5 %	29.5 %	28206
7313	1.6 %	14.1 %	17.1 %	49691
7314	0 %	3.1 %	63.1 %	41784
7315	0 %	8.4 %	35.5 %	39528
7316	12.7 %	5 %	27 %	40729
7317	6.8 %	15 %	37.7 %	36296
7318	1.5 %	1.2 %	38.3 %	49561
7319	4.5 %	0 %	36.9 %	36328
7320	0.6 %	0 %	57.7 %	56681

Figure 10: Results from HDR in salmon. The empty gray boxes on each side of FLAG represent cutsites. The numbers to the left of the sequence represent total reads of the specific sequence. FLAG sequences are in the middle of the two black vertical lines. Data from sample 7316 is shown. Figure taken from Geneious Prime software.

4.2 Modifying miR binding elements in 3'UTR of zebrafish genes *ifng* and *myd88*

miRs are known to regulate gene expression by binding to miR binding sites in the 3'UTRs of mRNAs. In most cases, this interaction leads to suppressed expression. Mutate the miR binding sites could be a way to increase the expression of genes important for immune function, since this would inhibit the miR to bind to its 3'UTR binding site. To investigate this, we searched for immune genes with few miR binding sites and early expression (<5dpf). We identified genes with miR 3'UTR binding sites associated with immune response in Atlantic salmon using Table 2 and 3 in Andreassen and Høyheim (2017). One gene, *ifng*, was chosen as it has only one miR binding site in zebrafish and the same miR present in salmon. Another gene of interest, *myd88*, was chosen due to having only three miR target sites, and being expressed earlier than 5 dpf in zebrafish. We selected these two genes, *ifng* and *myd88*, and their respective miR (*miR-223* and *miR-144*) for further studies.

4.2.1 *ifng* and *myd88*

The *ifng* gene plays a critical role in the body's defense against infections and has important functions in regulating immune responses and maintaining cellular homeostasis. In the 3'UTR of *ifng* we found only one conserved miR binding site, which is also present in salmon. To edit the *miR-223* target site we designed three gRNA for Cas12 (one cutting in the middle of the target site and two on either side). Two gRNA with Cas9 were also designed to cut on both sides of the *miR-223*. The *myd88* gene acts as an adapter protein in TLR signaling pathways, which identify invading pathogens and is a key component of the immune system. To edit the *myd88 miR-144* target site we designed three gRNAs for Cas9 (one cutting in the middle of the target site and two on either side of the target site). Two gRNA were also designed to cut on both sides of *miR-144*.

Zebrafish eggs (n=200-250) were injected for each of the six groups; (I) *ifng* target site with one gRNA cutting in the middle of the target site, (II) *ifng* target site L+R with one left and one right gRNA cutting on both sides of the target site to remove the whole target site, (III) *miR-223* L+R with one gRNA on each side of the *miR-223* to remove the whole miR, (IV) *myd88* target site with one gRNA cutting in the middle of the targetsite, (V) *myd88* target site L+R with one gRNA on each side of the target site cutting out the whole target site and (VI) miR144 L+R with one left and one right gRNA on each side of the miR cutting out the whole miR. Cas12 was used for the *ifng* target site and the *ifng* target site L+R groups due to being more suitable as the target site was located in T´ rich area, while the rest of the groups were injected with Cas9. All groups were injected with gRNA targeting *slc45a2* for easy visual confirmation (Irion, 2014). At 5 dpf, around eight injected individuals with albino phenotype from each group were sampled for pre-screening by sanger sequencing (Figure 11 (1)), together with one injected individual without albino phenotype and one non-injected control (Figure 11 (2)). There were no significant differences in mortality or deformities in the injected groups when compared to the control groups.

Figure 11: Albino and pigmented zebrafish larvae from *myd88* injections. (1) Albino phenotype and (2) control, 5 dpf.

4.2.2 Sanger sequencing

To determine the effectiveness of the gRNAs, we initially conducted a screen using sanger sequencing. The sanger sequencing gave an indication whether the gRNA work or not based on the appearance of the sequence after the cut site. If the sequence is similar to the reference sequence with no or minimal "noise" in the sequence up until cutsite, and then becomes unreadable, i.e made up from "N"s, , it is an indication of an indel at the cut-site (Figure 12). Indel size can vary and the sequence beyond the cut site may be a combination of different sequences. The result from the *ifng* target site (Figure 12 a)) showed only mutation in 2 out of 9 individuals, while *ifng* target site L+R revealed a mutation in 7 out of 8 individuals (Figure 12 c)). 5 of 8 individuals were mutated in *myd88* target site (Figure 12 e)), while injections with *myd88* target site L+R did not give any mutations (Figure 12 g)). We did not go any further with *myd88* target site L+R. The sanger results did not produce any readable sequences for *miR-223* and *miR-144.*

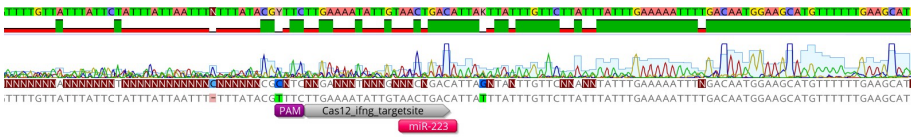

a) *ifng* target site mutated

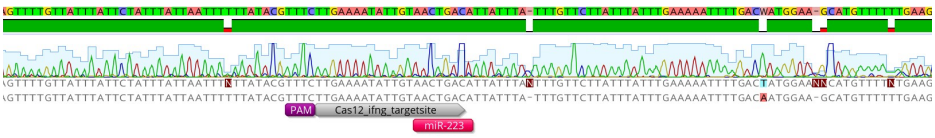

b) *ifng* target site control

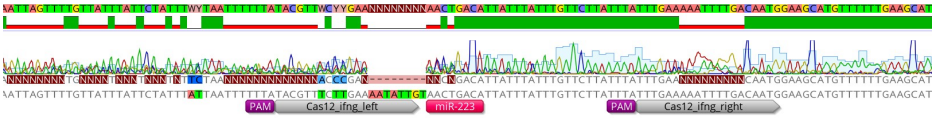

c) *ifng* target site L+R mutated

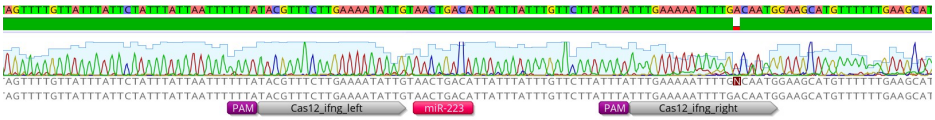

d) *ifng* target site L+R control

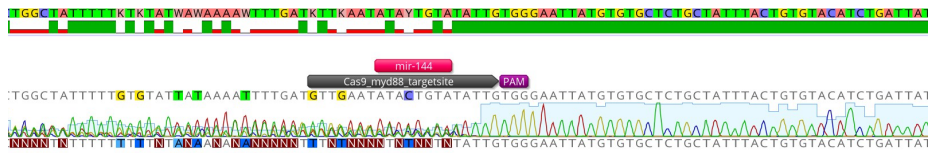

e) *myd88* target site mutated

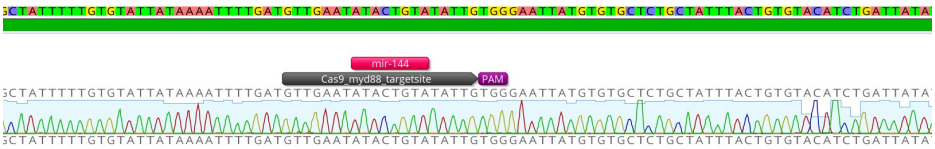

f) *myd88* target site control

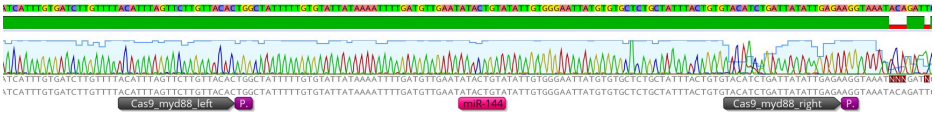

g) *myd88* target site L+R

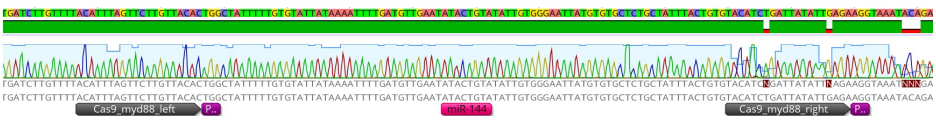

h) *myd88* target site L+R control

Figure 12: Sanger results from gRNA targeting *ifng* and *myd88*, zebrafish injections. Cut out from sanger sequencing results in Geneious Prime software, including the different injected groups. gRNA are colored in gray, with PAM sites for the gRNA colored in purple and miR target sites colored in pink. No data for *miR-223* and *miR-144*.

4.2.3 MiSeq

Based on the sanger sequencing result we concluded that *myd88* target site L+R gRNAs did not work, or worked with too low efficiency to be used for functional studies. The other five of the six injected groups in zebrafish (*myd88* target site L+R not included) were sent to MiSeq deep sequencing to determine the mutations efficiency in greater detail. Only sequence variants with 500 or more reads were included in the results.

4.2.3.1 *ifng*

The *ifng* target site showed an average of 11.5% mutation rate (Table 18), while cutting on the left side of target site (Table 19) revealed a high mutation rate of 67.2% on average, with three samples over 90%. The efficiency of the gRNA on the right side of the target site was notably lower compared to the left gRNA, and resulted in mutation in only two of the samples with the highest observed mutation value being 7.6%.

Table 18: Mutation *ifng* target site, MiSeq results.

Sample	% indels
101	35 %
102	18 %
103	5.6 %
104	4.1 %
105	11.1 %
106	3.4 %
107	5.5 %
108	9 %

Table 19: Mutation *ifng* target site L+R, MiSeq results. Samples from group *ifng* target site L+R where the two different gRNAs are separated to find their individual efficiency. No data for sample 604.

Sample	% L indels	% R indels	Total reads
601	88.3 %	7.6 %	138723
602	29.6 %	0 %	384367
603	54 %	0 %	231722
604	-	-	-
605	94.4 %	1.7 %	341193
606	100 %	0 %	6187
607	12.3 %	0 %	351196
608	91.7 %	0 %	247892

4.2.3.2 *miR-223*

The gRNA cutting on the left side of the *miR-223* exhibited poor effectiveness, as only one sample (703) had detectable indels in 0.4% of the reads (Table 20). On the other hand, the right gRNA demonstrated marginally better efficiency, with an average of 2.4%.

Table 20: Mutation *miR-223* L+R, MiSeq results. Left and right gRNAs on each side of *miR-223* are separated to calculate their individual efficiency.

Sample	% L indels	% R indels	Total reads
701	0 %	2.2 %	138863
702	0 %	1.3 %	127024
703	0.4 %	2 %	127717
704	0 %	0.5 %	95327
705	0 %	5.6 %	111546
706	0 %	6.6 %	109089
707	0 %	0.8 %	93164
708	0 %	0 %	58619

4.2.3.3 *myd88*

The gRNA targeting the *myd88* target site showed very high efficiency, as indicated by three samples exhibiting over 80% mutation rate, with the highest at 99.5% and an average of 67% mutation (Table 21). *myd88* target site group had the most consistent high mutation levels, and therefore being a natural group for further investigations.

Table 21: Mutation *myd88* target site, MiSeq results.

Sample	% indels
401	80.7 %
402	77.4 %
403	47.2 %
404	88.5 %
405	64 %
406	51.5 %
407	42.9 %
408	99.5 %

4.2.3.4 *miR-144*

The final group sent for MiSeq deep sequencing was injected with gRNA targeting *miR-144* L+R. Similar to the *miR-223* group, these injections resulted in one gRNA working while the other did not. The left gRNA targeting *miR-144* only showed mutations in two of the samples (Table 22). However, the right gRNA showed a high mutation frequency for all the samples with an average of 61.6%. None of the two miR groups (*miR-223* and *miR-144*) were further studied in this thesis.

Table 22: Mutation *miR-144* L+R, MiSeq results. Left and right gRNAs on each side of *miR-144* are separated to calculate their individual efficiency.

Sample	% L indels	% R indels	Total reads
501	0 %	70.7 %	133219
502	1.4 %	92.8 %	158770
503	2.4 %	85.2 %	127380
504	0 %	56.3 %	233508
505	0 %	40.9 %	238481
506	0 %	41.6 %	157870
507	0 %	35.5 %	270829
508	0 %	69.9 %	3628

4.2.4 qPCR

A mutated miR binding site can affect the mRNA stability and with the result from sequencing, we wanted to study the mRNA quantity by qPCR. To confirm the effect of the *myd88* KO we ran another injection with *myd88*, and extracted RNA from six injected individuals and six controls. First we ran a standard curve for the target gene (*myd88*) and the housekeeping genes (*elf1a* and *tuba1c*) to determine their efficiency (Figure 13). The efficiency should be between 90 - 110 %, where the housekeeping gene, *tuba1c*, had a bit lower efficiency at 84.9%. Figure 14 displays the anticipated qPCR result where samples inside the individual genes show a range of one cycle. While the result in the injected samples in Figure 15 display a broad spread in the

number of cycles between different extremes when expecting them to be aligned. Results of injected samples with the housekeeping gene *elfa1a* demonstrated a significant range, spanning from 14 to 36 cycles. Injected samples with the housekeeping gene *tuba1c* also showed a huge span in cycles, varying from 20 to 37 cycles. In contrast, the injected samples with *myd88* exhibit a less pronounced spread, with individual samples ranging from 22 to 26 cycles. Due to the extensive variability observed among samples within the different genes for the injected group, the wide range makes it difficult to rely on the results compared to the controls. Consequently, we decided to investigate the integrity of the RNA using Agilent Bioanalyzer.

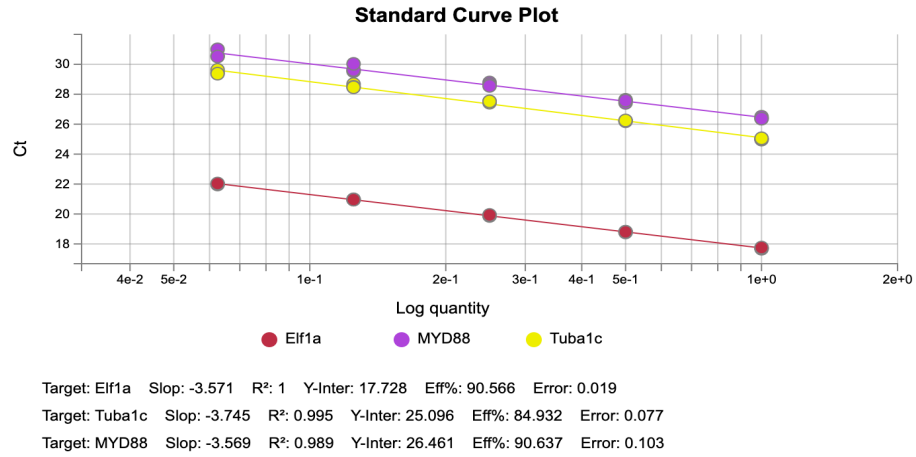

Figure 13: Standard curve for target gene (*myd88*) and housekeeping genes (*elf1a* and *tuba1c*). Testing the qPCR primers with standard curve. Ct (threshold cycle) against the logarithm of the starting template concentration. Figure taken from Design and Analysis Software.

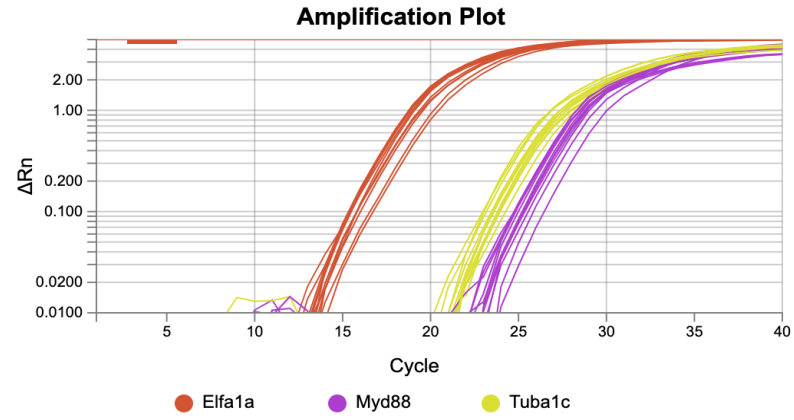

Figure 14: qPCR amplification plot for controls. Each line represents an individual sample (sample 1207-1212), fluorescent signal (ΔRn) against the number of PCR cycles. During the exponential phase, the PCR product doubles per cycle. The color represents which gene the sample contains. Figure taken from Design and Analysis Software.

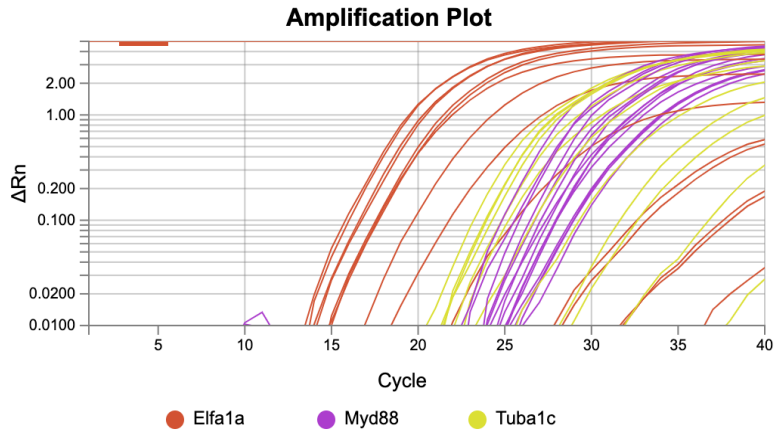

Figure 15: qPCR amplification plot for *myd88* injections. Each line represents an individual sample (sample 1201-1206), fluorescent signal (ΔRn) against the number of PCR cycles. During the exponential phase, the PCR product doubles per cycle. The color represents which gene the sample contains. Figure taken from Design and Analysis Software.

4.2.5 Agilent Bioanalyzer

To find the reason for extensive variability between the samples we chose to redo the injections, but with extended controls. We therefore did another round of injections with *myd88* gRNA, dH_2O, albino gRNA, and uninjected controls. The zebrafish larvae were sampled at 5 dpf in pools of 13 individuals from the group injected with albino gRNA or dH_2O, and pools of 17 individuals injected with the *myd88* gRNA. The different number of individuals in the pools are due to the amount of albino phenotype and survival in the different petri dishes. RNA was extracted, and to check the RNA quality, the samples were run through the Agilent Bioanalyzer. All of the samples injected with *myd88* had RIN value under 8, with lowest of 3.4 and highest at 6.8 (Figure 16). RIN values for injected groups with dH_2O and albino together with controls were of satisfying quality (Figure 17). Gel on Figures 16 and 17 show how insufficient the group injected with *myd88* was with a lot of fragments in different sizes, indicating degradation. This shows that injection in itself doesn't cause the degradation, nor the CRISPR/Cas9, but indicates that injections of the *myd88* gRNA is the cause.

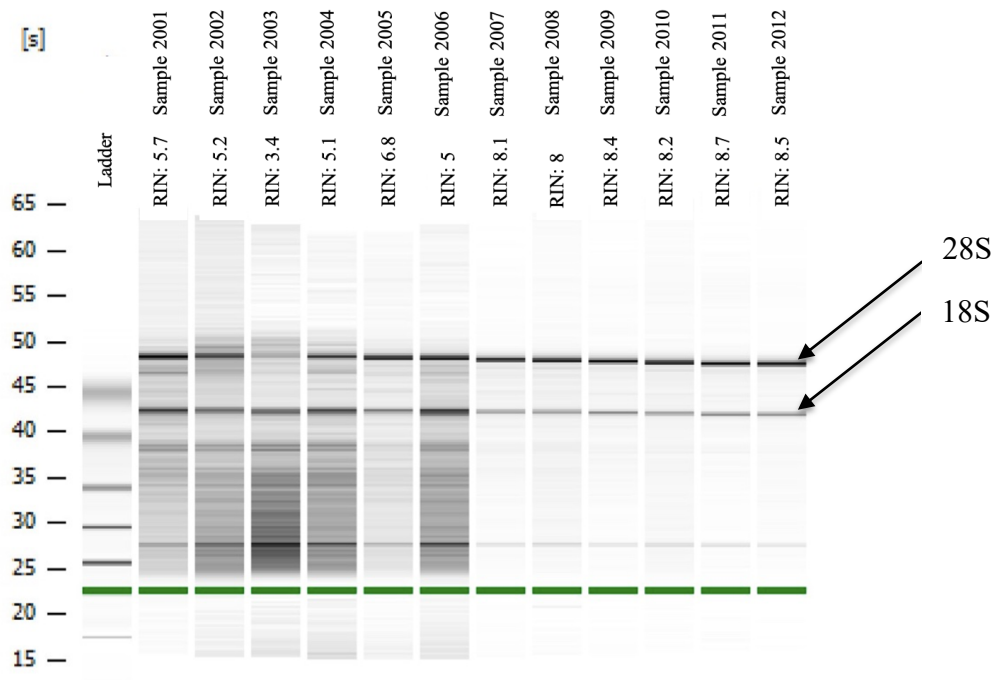

Figure 16: Gel displaying injected (*myd88)* and control RNA samples from Agilent Bioanalyzer. Gel showing different fragments and their size in seconds, showing how many seconds it took before the band passed in front of the detector, on the left side. Ladder on the left is used as a reference, with bands on 200, 500, 1000, 2000, 4000 and 6000 bases. The green line is position of the marker added to the wells, and the software uses it as reference to align all samples. RIN values between gel and sample id. *myd88* injections in sample 2001-2006 and control sample 2007-2012.

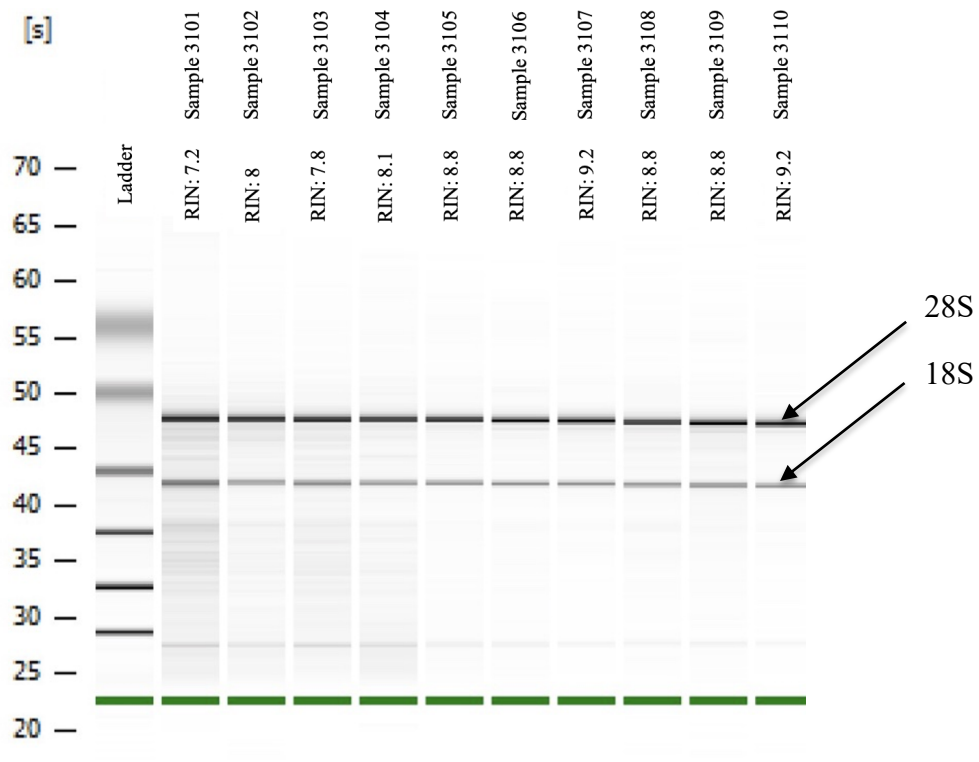

Figure 17: Gel displaying injected (albino and dH_2O*)* and control RNA samples from Agilent Bioanalyzer. Gel showing different fragments and their size in seconds, showing how many seconds it took before the band passed in front of the detector, on the left side. Ladder on the left is used as a reference, with bands on 200, 500, 1000, 2000, 4000 and 6000 bases. The green line is position of the marker added to the wells, and the software uses it as reference to align all samples. RIN values between gel and sample id. Injections only with albino gRNA in sample 3101-3104, injections with dH_2O in sample 3105+3106 and control sample 3107-3110.

5 Discussion

5.1 Base editing

To our knowledge, base editing has not been previously described and reported in salmon. As shown in this thesis, base editing was shown to have very high efficiency in converting a target base from C to T to induce a stop codon in the albino gene. The result from MiSeq deep sequencing revealed an 66.5% average efficiency of changing one base of the eight sampled larvae. All sampled individuals exhibit a high percentage of correct conversion. The individuals with the clearest albino phenotype were sampled first, and they also had the highest percentage of correct conversion at 89.1% (sample 6101) and 87% (sample 6102), respectively. Base editing has several benefits, one of them is that it contains a modified Cas9, which will not make a DSB in the DNA. This may significantly reduce the off-target effects, providing greater control over gene editing. Despite this promise of decreased off-target effects, we found examples of both by-stander edits, incorrect conversions, insert and deletions, indicating that this technology still has room for improvement. Another benefit with base editing is the possibility to change one amino acid or introduce a premature stop codon with high efficiency, and this can be useful for studying effects already in injected individuals in the F0 generation. On the other hand, this Cas9 gives indels despite that it should not give DSB.

5.2 Cas12 KO and KI

As with base editing, Cas12 has previously neither been described nor reported in salmon. Cas12, a more recent gene editing tool compared to Cas9, broadens the scope of gene editing by being able to make edits in locations where Cas9 is unable. Cas12 recognizes the PAM sequence of TTTV making it possible to make genetic changes in T´rich areas, where Cas9 has no PAM site. For CRISPR/Cas12 mediated KI, previous studies in zebrafish have shown that when using ODN, designed complementary to the target or the non-target strand, only the target ODN design worked (Moreno-Mateos et al., 2017). Therefore, in this study, we wanted to test both target and non-target ODN templates for CRISPR/Cas12 mediated HDR. Cas12 recognizes the PAM site on the non-target strand and binds to the target strand (opposite strand than the one with PAM site). Deep sequencing revealed that both target and non-target KI of FLAG did work, and with higher efficiency than expected. Target group had a perfect FLAG insert of 3.2% on average, with the highest occurrence of 34.3%. The non-target group had a

very high percentage of perfect FLAG insert of 6.7% on average, with the highest sample having as much as 54.9% perfect inserted FLAG sequences. Results from this study are similar to results obtained in a study done by Straume et al. (2020), using Cas9. Together with the high observed effect of perfect HDR, the KO effect was also very high for all samples. This is an indication of how efficient the Cas12 cutting tool is, with the average KO among all samples as high as 57.8%.

5.3 miR binding elements in 3´UTR in zebrafish

5.3.1 Zebrafish as a model

Zebrafish is a widely used model organism. Due to the prolonged generation time and limited availability of salmon eggs throughout the year, coupled with the space requirements, zebrafish can work as an excellent species for testing of new technology before implementing this in salmon. Genes chosen for this study (*ifng* and *myd88*) were selected for their early expression and few miR binding sites together with being immune genes. *ifng* being the gene of greatest interest as it only has one miR binding that is also found in salmon.

5.3.2 *ifng*

Injections of Cas12 protein, along with gRNA targeting the miR target site in *ifng*, were performed to influence the mRNA stability. One group of injections included only a single gRNA targeting the middle of the target sequence to disrupt it. MiSeq deep sequencing revealed that this approach was effective, resulting in varying levels of mutation in all sampled individuals, with the highest instance at 35%. Another group of injections involved one gRNA on each side of the target site trying to KO the entire miR binding site. For this approach to be successful, both of the gRNAs needed to work. Unfortunately, in this study, only the left gRNA was effective. The left gRNA had high efficiency, resulting in an average mutation rate of 67.2% according to MiSeq deep sequencing. The right gRNA showed low effectiveness with only mutation in two of the samples, with highest occurrence at 7.6%. This group holds potential for further studies, particularly by designing new gRNA cutting on the right side of the target site, and achieving KO of the whole target site.

Additionally, the prioritization of *ifng* was influenced by its expression. The gel indicated that *ifng* was not expressed at 5 dpf, despite initial information at The Zebrafish Information Network (ZFIN, www.zfin.org) suggesting early developmental expression. Further studies should be conducted to identify when *ifng* are expressed. Nevertheless, *ifng* remains an interesting gene to follow up due to its possession of a single miR target site as well as having target site in salmon, which is the ultimate goal, to directly apply this to salmon.

5.3.3 *miR-223* and *miR-144*

Each miR has multiple miR target sites, and by KO a specific miR target site in the 3´UTR of a specific gene, only that particular gene is affected. That gene should, along with other genes having binding sites for this miR, also be affected if the miR itself is KO'ed. We therefore tried to KO *miR-223* and *miR-144* to see if this would lead to increased expression of *ifng* and *myd88*, respectively. For both injected groups, *miR-223* and *miR-144*, Cas9 protein and one gRNA on each side of the miR were injected into zebrafish eggs. MiSeq deep sequencing of *miR-223* demonstrated low efficiency for both gRNAs, with the left gRNA being ineffective and the right gRNA having an average mutation rate of 2.4%. Results from *miR-144* revealed that the left gRNA was not efficient, while in contrast, the right gRNA exhibited a very high efficiency with average mutation rate at 61.6%.

5.3.4 *myd88*

Injections with Cas9 protein and gRNA targeting the *miR-144* target site in the 3'UTR of *myd88* showed 67% mutation on average, from data obtained from MiSeq deep sequencing. The highest mutation observed was at 99.5%, and only two samples had under 50% mutation rate (42.9% and 47.2%). The high mutation rate for this gRNA gave reasons to carry out experiments to see if the *myd88* mRNA levels were affected.

If the CRISPR technology actually disrupts the miR binding site in the 3'UTR of *myd88* mRNA, it could potentially lead to increased stability and translation of the *myd88* mRNA. This, in turn, could result in increased *myd88* protein expression, which plays a crucial role in the innate immune response. Increased *myd88* expression could also potentially lead to increased cellular stress and RNA degradation. This is because *myd88* is involved in signaling

pathways that activate inflammatory responses, and chronic inflammation has been shown to contribute to cellular stress and RNA degradation (Uchida et al., 2019). Our observation of RNA degradation is not due to either CRISPR nor the injections itself, as checked in the groups only injected with albino gRNA and dH_2O. Therefore, it is possible that the CRISPR KO of the *myd88* miR binding site could impact the mRNA stability and contribute to the observed RNA degradation in the injected zebrafish samples, as demonstrated by the Agilent Bioanalyzer results.

5.4 Conclusion and further perspectives

Work in this thesis has provided crucial advancement in the field of CRISPR technology by base editing and Cas12 (both KO and KI), which has not been previously reported in salmon, and will be important tools for further studies towards a more robust salmon. The findings from the zebrafish experiment in this thesis can be implemented for future studies in salmon, highlighting the utility of zebrafish as a model organism for salmon research. One of the major advantages of using zebrafish in this study was the ability to perform multiple injections, which would have been too time consuming if conducted in salmon. Although there were varying results in the effect of the different gRNA, we still believe in the strategy for disrupting miR target sites is valid, and this project will continue with further investigations. In this project we tested out several hypotheses in zebrafish, and possibly making a model for salmon. Although, *myd88* may not be as good a model for salmon, as KO of the target site in 3´UTR in mRNA seemingly leads to RNA degradation and the gene being important for early immune response. *ifng* on the other hand, could still be a great target, the gRNA used to KO the target site showed promising results, and we have strong belief in its potential for further studies, including KO of the target site in salmon.

6 References

Adli, M. (2018). The CRISPR tool kit for genome editing and beyond. *Nature communications*, *9*(1), 1911. https://doi.org/https://doi.org/10.1038/s41467-018-04252-2

Andreassen, R., & Høyheim, B. (2017). miRNAs associated with immune response in teleost fish. *Developmental & Comparative Immunology*, *75*, 77-85. https://doi.org/https://doi.org/10.1016/j.dci.2017.02.023

Anzalone, A. V., Koblan, L. W., & Liu, D. R. (2020). Genome editing with CRISPR–Cas nucleases, base editors, transposases and prime editors. *Nature biotechnology*, *38*(7), 824-844. https://doi.org/https://doi.org/10.1038/s41587-020-0561-9

Bartel, D. P. (2018). Metazoan micrornas. *Cell*, *173*(1), 20-51. https://doi.org/https://doi.org/10.1016/j.cell.2018.03.006

Brouns, S. J. J., Jore, M. M., Lundgren, M., Westra, E. R., Slijkhuis, R. J. H., Snijders, A. P. L., Dickman, M. J., Makarova, K. S., Koonin, E. V., & Van Der Oost, J. (2008). Small CRISPR RNAs guide antiviral defense in prokaryotes. *Science*, *321*(5891), 960-964. https://doi.org/10.1126/science.1159689

Edvardsen, R. B., Leininger, S., Kleppe, L., Skaftnesmo, K. O., & Wargelius, A. (2014). Targeted mutagenesis in Atlantic salmon (Salmo salar L.) using the CRISPR/Cas9 system induces complete knockout individuals in the F0 generation. *PLoS One*, *9*(9), e108622. https://doi.org/https://doi.org/10.1371/journal.pone.0108622

FAO. (2022). *The State of World Fisheries*.

Gagnon, J. A., Valen, E., Thyme, S. B., Huang, P., Ahkmetova, L., Pauli, A., Montague, T. G., Zimmerman, S., Richter, C., & Schier, A. F. (2014). Efficient mutagenesis by Cas9 protein-mediated oligonucleotide insertion and large-scale assessment of single-guide RNAs. *PLoS One*, *9*(5), e98186. https://doi.org/https://doi.org/10.1371/journal.pone.0098186

Gaj, T., Gersbach, C. A., & Barbas, C. F. (2013). ZFN, TALEN, and CRISPR/Cas-based methods for genome engineering. *Trends in biotechnology*, *31*(7), 397-405. https://doi.org/https://doi.org/10.1016/j.tibtech.2013.04.004

Garlock, T., Asche, F., Anderson, J., Bjørndal, T., Kumar, G., Lorenzen, K., Ropicki, A., Smith, M. D., & Tveterås, R. (2020). A Global Blue Revolution: Aquaculture Growth Across Regions, Species, and Countries. *Reviews in Fisheries Science & Aquaculture*, *28*(1), 107-116. https://doi.org/https://doi.org/10.1080/23308249.2019.1678111

Gratacap, R. L., Wargelius, A., Edvardsen, R. B., & Houston, R. D. (2019). Potential of genome editing to improve aquaculture breeding and production. *Trends in Genetics*, *35*(9), 672-684. https://doi.org/https://doi.org/10.1016/j.tig.2019.06.006

Grimholt, U., Fosse, J. H., & Sundaram, A. Y. M. (2020). Selective stimulation of duplicated Atlantic salmon MHC pathway genes by interferon-gamma. *Frontiers in Immunology*, *11*, 571650. https://doi.org/https://doi.org/10.3389/fimmu.2020.571650

Herbomel, P., Thisse, B., & Thisse, C. (1999). Ontogeny and behaviour of early macrophages in the zebrafish embryo. *Development*, *126*(17), 3735-3745. https://doi.org/https://doi.org/10.1242/dev.126.17.3735

Howe, K., Clark, M. D., Torroja, C. F., Torrance, J., Berthelot, C., Muffato, M., Collins, J. E., Humphray, S., McLaren, K., & Matthews, L. (2013). The zebrafish reference genome sequence and its relationship to the human genome. *Nature*, *496*(7446), 498-503. https://doi.org/https://doi.org/10.1038/nature12111

Hvas, M., Folkedal, O., & Oppedal, F. (2021). Fish welfare in offshore salmon aquaculture. *Reviews in Aquaculture*, *13*(2), 836-852. https://doi.org/ https://doi.org/10.1111/raq.12501

Ishino, Y., Shinagawa, H., Makino, K., Amemura, M., & Nakata, A. (1987). Nucleotide sequence of the iap gene, responsible for alkaline phosphatase isozyme conversion in Escherichia coli, and identification of the gene product. *Journal of bacteriology*, *169*(12), 5429-5433. https://doi.org/https://doi.org/10.1128/jb.169.12.5429-5433.1987

Iversen, A., Asche, F., Hermansen, Ø., & Nystøyl, R. (2020). Production cost and competitiveness in major salmon farming countries 2003–2018. *Aquaculture*, *522*. https://doi.org/https://doi.org/10.1016/j.aquaculture.2020.735089

Kantor, A., McClements, M. E., & MacLaren, R. E. (2020). CRISPR-Cas9 DNA base-editing and prime-editing. *International journal of molecular sciences*, *21*(17), 6240. https://doi.org/https://doi.org/10.3390/ijms21176240

Kleppe, L., Andersson, E., Skaftnesmo, K. O., Edvardsen, R. B., Fjelldal, P. G., Norberg, B., Bogerd, J., Schulz, R. W., & Wargelius, A. (2017). Sex steroid production associated with puberty is absent in germ cell-free salmon. *Scientific Reports*, *7*(1), 1-11. https://doi.org/https://doi.org/10.1038/s41598-017-12936-w

Marraffini, L. A., & Sontheimer, E. J. (2008). CRISPR interference limits horizontal gene transfer in staphylococci by targeting DNA. *Science*, *322*(5909), 1843-1845. https://doi.org/DOI: 10.1126/science.1165771

Moreno-Mateos, M. A., Fernandez, J. P., Rouet, R., Vejnar, C. E., Lane, M. A., Mis, E., Khokha, M. K., Doudna, J. A., & Giraldez, A. J. (2017). CRISPR-Cpf1 mediates efficient homology-directed repair and temperature-controlled genome editing. *Nature communications*, *8*(1), 2024. https://doi.org/https://doi.org/10.1038/s41467-017-01836-2

Parichy, D. M., Elizondo, M. R., Mills, M. G., Gordon, T. N., & Engeszer, R. E. (2009). Normal table of postembryonic zebrafish development: staging by externally visible anatomy of the living fish. *Developmental dynamics*, *238*(12), 2975-3015. https://doi.org/https://doi.org/10.1002/dvdy.22113

Pettersen, J. M., Osmundsen, T., Aunsmo, A., Mardones, F. O., & Rich, K. M. (2015). Controlling emerging infectious diseases in salmon aquaculture. *Rev Sci Tech*, *34*(3), 923-938. https://doi.org/10.20506/rst.34.3.2406

Pickar-Oliver, A., & Gersbach, C. A. (2019). The next generation of CRISPR–Cas technologies and applications. *Nature reviews Molecular cell biology*, *20*(8), 490-507. https://doi.org/https://doi.org/10.1038/s41580-019-0131-5

Ruan, J., Xu, J., Chen-Tsai, R. Y., & Li, K. (2017). Genome editing in livestock: Are we ready for a revolution in animal breeding industry? *Transgenic research*, *26*, 715-726. https://doi.org/https://doi.org/10.1007/s11248-017-0049-7

Saber Sichani, A., Ranjbar, M., Baneshi, M., Torabi Zadeh, F., & Fallahi, J. (2022). A Review on Advanced CRISPR-Based Genome-Editing Tools: Base Editing and Prime Editing. *Molecular Biotechnology*, 1-12. https://doi.org/https://doi.org/10.1007/s12033-022-00639-1

Straume, A. H., Kjærner-Semb, E., Ove Skaftnesmo, K., Güralp, H., Kleppe, L., Wargelius, A., & Edvardsen, R. B. (2020). Indel locations are determined by template polarity in highly efficient in vivo CRISPR/Cas9-mediated HDR in Atlantic salmon. *Scientific Reports*, *10*(1), 409. https://doi.org/https://doi.org/10.1038/s41598-019-57295-w

Straume, A. H., Kjærner-Semb, E., Skaftnesmo, K. O., Güralp, H., Lillico, S., Wargelius, A., & Edvardsen, R. B. (2021). Single nucleotide replacement in the Atlantic salmon genome using CRISPR/Cas9 and asymmetrical oligonucleotide donors. *BMC genomics*, *22*, 1-8, Article 563. https://doi.org/https://doi.org/10.1186/s12864-021-07823-8

Streisinger, G., Walker, C., Dower, N., Knauber, D., & Singer, F. (1981). Production of clones of homozygous diploid zebra fish (Brachydanio rerio). *Nature*, *291*(5813), 293-296. https://doi.org/https://doi.org/10.1038/291293a0

Takeda, K., & Akira, S. (2004). Microbial recognition by Toll-like receptors. *Journal of dermatological science*, *34*(2), 73-82. https://doi.org/https://doi.org/10.1016/j.jdermsci.2003.10.002

Uchida, Y., Chiba, T., Kurimoto, R., & Asahara, H. (2019). Post-transcriptional regulation of inflammation by RNA-binding proteins via cis-elements of mRNAs. *The journal of biochemistry*, *166*(5), 375-382. https://doi.org/https://doi.org/10.1093/jb/mvz067

van der Vaart, M., van Soest, J. J., Spaink, H. P., & Meijer, A. H. (2013). Functional analysis of a zebrafish myd88 mutant identifies key transcriptional components of the innate immune system. *Disease models & mechanisms*, *6*(3), 841-854. https://doi.org/https://doi.org/10.1242/dmm.010843

Wargelius, A. (2019). Application of genome editing in aquatic farm animals: Atlantic salmon. *Transgenic research*, *8* (2), 101-105. https://doi.org/10.1007/s11248-019-00163-0

Wargelius, A., Leininger, S., Skaftnesmo, K. O., Kleppe, L., Andersson, E., Taranger, G. L., Schulz, R. W., & Edvardsen, R. B. (2016). Dnd knockout ablates germ cells and demonstrates germ cell independent sex differentiation in Atlantic salmon. *Scientific Reports*, *6*(1), 1-8. https://doi.org/https://doi.org/10.1038/srep21284

7 Appendix

Table A1: Primer sequences. Letters written in cursive indicates adapter sequence.

Primer	Sequence (5´- 3´)
*ifng*_MiSeq_F	*TCTTTCCCTACACGACGCTCTTCCGATCT*TCAGTGCCTAAAATGGTGTG
*ifng*_MiSeq_R	*TGGAGTTCAGACGTGTGCTCTTCCGATCT*GCATTTATTTAGTCATAGACTTTACC
*myd88*_MiSeq_F	*TCTTTCCCTACACGACGCTCTTCCGATCT*CACAAATCAAAACATCACTCAGC
*myd88*_MiSeq_R	*TGGAGTTCAGACGTGTGCTCTTCCGATCT*CTAACCAACAACAGAGAGAAAG
miR223_MiSeq_F	*TCTTTCCCTACACGACGCTCTTCCGATCT*TGACCTTCCTGCTGCAAACC
miR223_MiSeq_R	*TGGAGTTCAGACGTGTGCTCTTCCGATC*TGAGAGTAACAGGATCGCATGG
miR144_MiSeq_F	*TCTTTCCCTACACGACGCTCTTCCGATCT*GGTCAAATGTGATTTTAGATGC
miR144_MiSeq_R	*TGGAGTTCAGACGTGTGCTCTTCCGATC*TAGCAGAACCCTTACCATTAC
Alb1_MiSeq_F	*TCTTTCCCTACACGACGCTCTTCCGATCT*GGATTCTTCCTGTTGTGACACC
Alb1_MiSeq_R	*TGGAGTTCAGACGTGTGCTCTTCCGATCT*GAGGTTATTCCACGTATCTGATG
Cas12_Alb2_ex1_ MiSeq_F	*TCTTTCCCTACACGACGCTCTTCCGATCT*GCTATGTCCCTCCTCACAGG
Cas12_Alb2_ex1_ MiSeq_R	*TGGAGTTCAGACGTGTGCTCTTCCGATCT*GCTGATCAGCCACACAAGGC
*elf1a*_F	CTCCTCTTGGTCGCTTTGCT
*elf1a*_R	GCCTTCTGTGCAGACTTTGTGA
*tuba1c*_F	TGCCTCAATCTTGGACAGTG
*tuba1c*_R	TGGATGCCATGCTCAAGAC

Table A2: Contents of E3 clear.

NaCl	8.6g
$CaCL_2$	1.45g
$MgSO_4$	2.45g
KCl	0.38g
dH_2O	5dl

Table A3: Contents of E3 blue, embryo medium.

E3 stock	33ml
RO-water	2L
Methylene blue	2 drops
$NaHCO_3$	250mg

Table A4: gRNA sequences for base edit and Cas12 KO and KI. PAM sites are underlined.

gRNA	**Sequences (5´-3´)**
Base edit	GGCTCAGATCATCGTGGGGGCGG
Cas12_ODN	TTTGGAAGGGAATTTTGCTATGCG

Table A5: Colors referring to groups in Figure 7.

Sample	Name	Species	Sampled	Individual/pool	Analyzes	Mutation sanger
101	*ifng*_targetsite	*Danio rerio*	3dpf	individual	DNA extraction	yes
102	*ifng*_targetsite	*Danio rerio*	3dpf	individual	DNA extraction	no
103	*ifng*_targetsite	*Danio rerio*	3dpf	individual	DNA extraction	no
104	*ifng*_targetsite	*Danio rerio*	3dpf	individual	DNA extraction	no
105	*ifng*_targetsite	*Danio rerio*	3dpf	individual	DNA extraction	no
106	*ifng*_targetsite	*Danio rerio*	3dpf	individual	DNA extraction	no
107	*ifng*_targetsite	*Danio rerio*	3dpf	individual	DNA extraction	no
108	*ifng*_targetsite	*Danio rerio*	3dpf	individual	DNA extraction	no
109	*ifng*_targetsite	*Danio rerio*	3dpf	individual	DNA extraction	yes
110	*ifng*_targetsite_ control	*Danio rerio*	3dpf	individual	DNA extraction	no
601	*ifng*_targetsite_ L+R	*Danio rerio*	5dfp	individual	DNA extraction	L: yes R: no
602	*ifng*_targetsite_ L+R	*Danio rerio*	5dpf	individual	DNA extraction	L: no R: yes
603	*ifng*_targetsite_ L+R	*Danio rerio*	5dpf	individual	DNA extraction	L: yes R: no
604	*ifng*_targetsite_ L+R	*Danio rerio*	5dpf	individual	DNA extraction	L: yes R: yes
605	*ifng*_targetsite_ L+R	*Danio rerio*	5dpf	individual	DNA extraction	L: yes R: no
606	*ifng*_targetsite_ L+R	*Danio rerio*	5dpf	individual	DNA extraction	L: yes R: yes
607	*ifng*_targetsite_ L+R	*Danio rerio*	5dpf	individual	DNA extraction	L: no R: no
608	*ifng*_targetsite_ L+R	*Danio rerio*	5dpf	individual	DNA extraction	L: yes R: no
609	*ifng*_targetsite_ L+R_WT	*Danio rerio*	5dpf	individual	DNA extraction	no

610	*ifng*_targetsite_L+R_control	*Danio rerio*	5dpf	individual	DNA extraction	no
701	miR223	*Danio rerio*	5dpf	individual	DNA extraction	NaN
702	miR223	*Danio rerio*	5dpf	individual	DNA extraction	NaN
703	miR223	*Danio rerio*	5dpf	individual	DNA extraction	NaN
704	miR223	*Danio rerio*	5dpf	individual	DNA extraction	NaN
705	miR223	*Danio rerio*	5dpf	individual	DNA extraction	NaN
706	miR223	*Danio rerio*	5dpf	individual	DNA extraction	NaN
707	miR223	*Danio rerio*	5dpf	individual	DNA extraction	NaN
708	miR223	*Danio rerio*	5dpf	individual	DNA extraction	NaN
709	miR223_WT	*Danio rerio*	5dpf	individual	DNA extraction	NaN
710	miR223_control	*Danio rerio*	5dpf	individual	DNA extraction	NaN
401	*myd88*_targetsite	*Danio rerio*	5dpf	individual	DNA extraction	yes
402	*myd88*_targetsite	*Danio rerio*	5dpf	individual	DNA extraction	yes
403	*myd88*_targetsite	*Danio rerio*	5dpf	individual	DNA extraction	no
404	*myd88*_targetsite	*Danio rerio*	5dpf	individual	DNA extraction	yes
405	*myd88*_targetsite	*Danio rerio*	5dpf	individual	DNA extraction	yes
406	*myd88*_targetsite	*Danio rerio*	5dpf	individual	DNA extraction	no
407	*myd88*_targetsite	*Danio rerio*	5dpf	individual	DNA extraction	no
408	*myd88*_targetsite	*Danio rerio*	5dpf	individual	DNA extraction	yes
409	*myd88*_targetsite_WT	*Danio rerio*	5dpf	individual	DNA extraction	no

410	*myd88*_targetsite_control	*Danio rerio*	5dpf	individual	DNA extraction	no
301	*myd88*_targetsite_L+R	*Danio rerio*	5dpf	individual	DNA extraction	L: no R: no
302	*myd88*_targetsite_L+R	*Danio rerio*	5dpf	individual	DNA extraction	L: no R: no
303	*myd88*_targetsite_L+R	*Danio rerio*	5dpf	individual	DNA extraction	L: no R: no
304	*myd88*_targetsite_L+R	*Danio rerio*	5dpf	individual	DNA extraction	L: no R: no
305	*myd88*_targetsite_L+R	*Danio rerio*	5dpf	individual	DNA extraction	L: no R: no
306	*myd88*_targetsite_L+R	*Danio rerio*	5dpf	individual	DNA extraction	L: no R: no
307	*myd88*_targetsite_L+R	*Danio rerio*	5dpf	individual	DNA extraction	L: no R: no
307	*myd88*_targetsite_L+R	*Danio rerio*	5dpf	individual	DNA extraction	L: no R: no
309	*myd88*_targetsite_L+R_WT	*Danio rerio*	5dpf	individual	DNA extraction	no
310	*myd88*_targetsite_L+R_control	*Danio rerio*	5dpf	individual	DNA extraction	no
501	miR144	*Danio rerio*	5dpf	individual	DNA extraction	NaN
502	miR144	*Danio rerio*	5dpf	individual	DNA extraction	NaN
503	miR144	*Danio rerio*	5dpf	individual	DNA extraction	NaN
504	miR144	*Danio rerio*	5dpf	individual	DNA extraction	NaN
505	miR144	*Danio rerio*	5dpf	individual	DNA extraction	NaN
506	miR144	*Danio rerio*	5dpf	individual	DNA extraction	NaN
507	miR144	*Danio rerio*	5dpf	individual	DNA extraction	NaN
508	miR144	*Danio rerio*	5dpf	individual	DNA extraction	NaN
509	miR144_WT	*Danio rerio*	5dpf	individual	DNA extraction	NaN

510	miR144_control	*Danio rerio*	5dpf	individual	DNA extraction	NaN
1101	*ifng*_targetsite_L	*Danio rerio*	5dpf	individual	RNA extraction + cDNA	-
1102	*ifng*_targetsite_L	*Danio rerio*	5dpf	individual	RNA extraction + cDNA	-
1103	*ifng*_targetsite_L	*Danio rerio*	5dpf	individual	RNA extraction + cDNA	-
1104	*ifng*_targetsite_L	*Danio rerio*	5dpf	individual	RNA extraction + cDNA	-
1105	*ifng*_targetsite_L	*Danio rerio*	5dpf	individual	RNA extraction + cDNA	-
1106	*ifng*_targetsite_L	*Danio rerio*	5dpf	individual	RNA extraction + cDNA	-
1107	*ifng*_targetsite_L	*Danio rerio*	5dpf	individual	RNA extraction + cDNA	-
1108	*ifng*_targetsite_L	*Danio rerio*	5dpf	individual	RNA extraction + cDNA	-
1109	*ifng*_targetsite_L	*Danio rerio*	5dpf	individual	RNA extraction + cDNA	-
1110	*ifng*_targetsite_L	*Danio rerio*	5dpf	individual	RNA extraction + cDNA	-
1111	*ifng*_targetsite_L_control	*Danio rerio*	5dpf	individual	RNA extraction + cDNA	-
1112	*ifng*_targetsite_L_control	*Danio rerio*	5dpf	individual	RNA extraction + cDNA	-
1113	*ifng*_targetsite_L_control	*Danio rerio*	5dpf	individual	RNA extraction + cDNA	-
1114	*ifng*_targetsite_L_control	*Danio rerio*	5dpf	individual	RNA extraction + cDNA	-

1115	*ifng*_targetsite_L_control	*Danio rerio*	5dpf	individual	RNA extraction + cDNA	-
1116	*ifng*_targetsite_L_control	*Danio rerio*	5dpf	individual	RNA extraction + cDNA	-
1201	*myd88*_targetsite	*Danio rerio*	5dpf	individual	RNA extraction + cDNA + qPCR	-
1202	*myd88*_targetsite	*Danio rerio*	5dpf	individual	RNA extraction + cDNA + qPCR	-
1203	*myd88*_targetsite	*Danio rerio*	5dpf	individual	RNA extraction + cDNA + qPCR	-
1204	*myd88*_targetsite	*Danio rerio*	5dpf	individual	RNA extraction + cDNA + qPCR	-
1205	*myd88*_targetsite	*Danio rerio*	5dpf	individual	RNA extraction + cDNA + qPCR	-
1206	*myd88*_targetsite	*Danio rerio*	5dpf	individual	RNA extraction + cDNA + qPCR	-
1207	*myd88*_targetsite_control	*Danio rerio*	5dpf	individual	RNA extraction + cDNA + qPCR	-
1208	*myd88*_targetsite_control	*Danio rerio*	5dpf	individual	RNA extraction + cDNA + qPCR	-
1209	*myd88*_targetsite_control	*Danio rerio*	5dpf	individual	RNA extraction + cDNA + qPCR	-
1210	*myd88*_targetsite_control	*Danio rerio*	5dpf	individual	RNA extraction + cDNA + qPCR	-

1211	*myd88*_targetsite_control	*Danio rerio*	5dpf	individual	RNA extraction + cDNA + qPCR	-
1212	*myd88*_targetsite_control	*Danio rerio*	5dpf	individual	RNA extraction + cDNA + qPCR	-
2001	*myd88*_targetsite	*Danio rerio*	5dpf	pool	RNA isolation + Bioanalyzer	-
2002	*myd88*_targetsite	*Danio rerio*	5dpf	pool	RNA isolation + Bioanalyzer	-
2003	*myd88*_targetsite	*Danio rerio*	5dpf	pool	RNA isolation + Bioanalyzer	-
2004	*myd88*_targetsite	*Danio rerio*	5dpf	pool	RNA isolation + Bioanalyzer	-
2005	*myd88*_targetsite	*Danio rerio*	5dpf	pool	RNA isolation + Bioanalyzer	-
2006	*myd88*_targetsite	*Danio rerio*	5dpf	pool	RNA isolation + Bioanalyzer	-
2007	*myd88*_targetsite_control	*Danio rerio*	5dpf	pool	RNA isolation + Bioanalyzer	-
2008	*myd88*_targetsite_control	*Danio rerio*	5dpf	pool	RNA isolation + Bioanalyzer	-
2009	*myd88*_targetsite_control	*Danio rerio*	5dpf	pool	RNA isolation + Bioanalyzer	-
2010	*myd88*_targetsite_control	*Danio rerio*	5dpf	pool	RNA isolation + Bioanalyzer	-
2011	*myd88*_targetsite_control	*Danio rerio*	5dpf	pool	RNA isolation + Bioanalyzer	-
2012	*myd88*_targetsite_control	*Danio rerio*	5dpf	pool	RNA isolation + Bioanalyzer	-
3101	albino	*Danio rerio*	5dpf	pool	RNA isolation +	-

					Bioanalyzer	
3102	albino	*Danio rerio*	5dpf	pool	RNA isolation + Bioanalyzer	-
3103	albino	*Danio rerio*	5dpf	pool	RNA isolation + Bioanalyzer	-
3104	albino	*Danio rerio*	5dpf	pool	RNA isolation + Bioanalyzer	-
3105	dH_2O	*Danio rerio*	5dpf	pool	RNA isolation + Bioanalyzer	-
3106	dH_2O	*Danio rerio*	5dpf	pool	RNA isolation + Bioanalyzer	-
3107	control	*Danio rerio*	5dpf	pool	RNA isolation + Bioanalyzer	-
3108	control	*Danio rerio*	5dpf	pool	RNA isolation + Bioanalyzer	-
3109	control	*Danio rerio*	5dpf	pool	RNA isolation + Bioanalyzer	-
3110	control	*Danio rerio*	5dpf	pool	RNA isolation + Bioanalyzer	-
6101	base edit	*Salmo salar*	~700°D	individual	DNA isolation + MiSeq	-
6102	base edit	*Salmo salar*	~700°D	individual	DNA isolation + MiSeq	-
6103	base edit	*Salmo salar*	~700°D	individual	DNA isolation + MiSeq	-
6104	base edit	*Salmo salar*	~700°D	individual	DNA isolation + MiSeq	-
6105	base edit	*Salmo salar*	~700°D	individual	DNA isolation + MiSeq	-
6106	base edit	*Salmo salar*	~700°D	individual	DNA isolation +	-

					MiSeq	
6107	base edit	*Salmo salar*	~700°D	individual	DNA isolation + MiSeq	-
6108	base edit	*Salmo salar*	~700°D	individual	DNA isolation + MiSeq	-
7201	target	*Salmo salar*	~700°D	individual	DNA isolation + MiSeq	-
7201	target	*Salmo salar*	~700°D	individual	DNA isolation + MiSeq	-
7203	target	*Salmo salar*	~700°D	individual	DNA isolation + MiSeq	-
7204	target	*Salmo salar*	~700°D	individual	DNA isolation + MiSeq	-
7205	target	*Salmo salar*	~700°D	individual	DNA isolation + MiSeq	-
7206	target	*Salmo salar*	~700°D	individual	DNA isolation + MiSeq	-
7207	target	*Salmo salar*	~700°D	individual	DNA isolation + MiSeq	-
7208	target	*Salmo salar*	~700°D	individual	DNA isolation + MiSeq	-
7209	target	*Salmo salar*	~700°D	individual	DNA isolation + MiSeq	-
7210	target	*Salmo salar*	~700°D	individual	DNA isolation + MiSeq	-
7211	target	*Salmo salar*	~700°D	individual	DNA isolation + MiSeq	-
7212	target	*Salmo salar*	~700°D	individual	DNA isolation + MiSeq	-
7213	target	*Salmo salar*	~700°D	individual	DNA isolation +	-

					MiSeq	
7214	target	*Salmo salar*	~700°D	individual	DNA isolation + MiSeq	-
7215	target	*Salmo salar*	~700°D	individual	DNA isolation + MiSeq	-
7216	target	*Salmo salar*	~700°D	individual	DNA isolation + MiSeq	-
7217	target	*Salmo salar*	~700°D	individual	DNA isolation + MiSeq	-
7218	target	*Salmo salar*	~700°D	individual	DNA isolation + MiSeq	-
7219	target	*Salmo salar*	~700°D	individual	DNA isolation + MiSeq	-
7220	target	*Salmo salar*	~700°D	individual	DNA isolation + MiSeq	-
7221	target	*Salmo salar*	~700°D	individual	DNA isolation + MiSeq	-
7222	target	*Salmo salar*	~700°D	individual	DNA isolation + MiSeq	-
7223	target	*Salmo salar*	~700°D	individual	DNA isolation + MiSeq	-
7224	target	*Salmo salar*	~700°D	individual	DNA isolation + MiSeq	-
7225	target	*Salmo salar*	~700°D	individual	DNA isolation + MiSeq	-
7226	target	*Salmo salar*	~700°D	individual	DNA isolation + MiSeq	-
7227	target	*Salmo salar*	~700°D	individual	DNA isolation + MiSeq	-
7228	target_control	*Salmo salar*	~700°D	individual	DNA isolation +	-

					MiSeq	
7301	non-target	*Salmo salar*	~700°D	individual	DNA isolation + MiSeq	-
7302	non-target	*Salmo salar*	~700°D	individual	DNA isolation + MiSeq	-
7303	non-target	*Salmo salar*	~700°D	individual	DNA isolation + MiSeq	-
7304	non-target	*Salmo salar*	~700°D	individual	DNA isolation + MiSeq	-
7305	non-target	*Salmo salar*	~700°D	individual	DNA isolation + MiSeq	-
7306	non-target	*Salmo salar*	~700°D	individual	DNA isolation + MiSeq	-
7307	non-target	*Salmo salar*	~700°D	individual	DNA isolation + MiSeq	-
7308	non-target	*Salmo salar*	~700°D	individual	DNA isolation + MiSeq	-
7309	non-target	*Salmo salar*	~700°D	individual	DNA isolation + MiSeq	-
7310	non-target	*Salmo salar*	~700°D	individual	DNA isolation + MiSeq	-
7311	non-target	*Salmo salar*	~700°D	individual	DNA isolation + MiSeq	-
7312	non-target	*Salmo salar*	~700°D	individual	DNA isolation + MiSeq	-
7313	non-target	*Salmo salar*	~700°D	individual	DNA isolation + MiSeq	-
7314	non-target	*Salmo salar*	~700°D	individual	DNA isolation + MiSeq	-
7315	non-target	*Salmo salar*	~700°D	individual	DNA isolation +	-

					MiSeq	
7316	non-target	*Salmo salar*	~700°D	individual	DNA isolation + MiSeq	-
7317	non-target	*Salmo salar*	~700°D	individual	DNA isolation + MiSeq	-
7318	non-target	*Salmo salar*	~700°D	individual	DNA isolation + MiSeq	-
7319	non-target	*Salmo salar*	~700°D	individual	DNA isolation + MiSeq	-
7320	non-target	*Salmo salar*	~700°D	individual	DNA isolation + MiSeq	-
7321	non-target_control	*Salmo salar*	~700°D	individual	DNA isolation + MiSeq	-